# ACCELERATED DISTRIBUTION DEMONSTRATION SYSTEM

REGULATORY INFORMATION DISTRIBUTION SYSTEM (RIDS)

ACCESSION NBR:8911030081 DOC.DATE: 89/10/26 NOTARIZED: NO DOCKET #
FACIL:50-275 Diablo Canyon Nuclear Power Plant, Unit 1, Pacific Ga 05000275
50-323 Diablo Canyon Nuclear Power Plant, Unit 2, Pacific Ga 05000323
AUTH.NAME AUTHOR AFFILIATION
SHIFFER,J.D. Pacific Gas & Electric Co.
RECIP.NAME RECIPIENT AFFILIATION
Document Control Branch (Document Control Desk)

See Rpt.

SUBJECT: Forwards response to action items from 890616-17 long term seismic program fragility meeting.

DISTRIBUTION CODE: D031D COPIES RECEIVED:LTR 1 ENCL 1 SIZE: 84
TITLE: Diablo Canyon Long-Term Seismic Program

NOTES:

| | RECIPIENT ID CODE/NAME | COPIES LTTR | COPIES ENCL | RECIPIENT ID CODE/NAME | COPIES LTTR | COPIES ENCL |
|---|---|---|---|---|---|---|
| | PD5 LA | 1 | 0 | PD5 PD | 5 | 5 |
| | ROOD,H | 1 | 1 | | | |
| INTERNAL: | ACRS | 6 | 6 | ADM/LFMB | 1 | 0 |
| | NRR ASHAR,H | 1 | 1 | NRR BAGCHI,G | 1 | 1 |
| | NRR JENG,D | 1 | 1 | NRR PICHUMANI,R | 1 | 1 |
| | NRR REITER,L | 1 | 1 | NRR ROTHMAN,R | 1 | 1 |
| | NRR/DEST/ADS 7E | 1 | 1 | NRR/PMAS/ILRB12 | 1 | 1 |
| | NUDOCS-ABSTRACT | 1 | 1 | OGC/HDS2 | 1 | 0 |
| | REG FILE 01 | 1 | 1 | RES CHOKSHI,N | 1 | 1 |
| | RES MCMULLEN,R | 1 | 1 | | | |
| EXTERNAL: | LPDR | 1 | 1 | NRC PDR | 1 | 1 |
| | NSIC | 1 | 1 | | | |

TOTAL NUMBER OF COPIES REQUIRED: LTTR 30 ENCL 27

MAD
cc

R I D S / A D D S

R I D S / A D D S

Pacific Gas and Electric Company

77 Beale Street
San Francisco, CA 94106
415/972-7000
TWX 910-372-6587

James D. Shiffer
Vice President
Nuclear Power Generation

October 26, 1989

PG&E Letter No. DCL-89-269

U.S. Nuclear Regulatory Commission
ATTN: Document Control Desk
Washington, D.C. 20555

Re: Docket No. 50-275, OL-DPR-80
Docket No. 50-323, OL-DPR-82
Diablo Canyon Units 1 and 2
Response to Action Items from the Long Term Seismic Program
Fragility Meeting, June 16-17, 1989

Gentlemen:

PG&E's responses to Action Items 1-5, 7, 8, and 13 related to fragility analysis identified in Enclosure 4 of the NRC letter to PG&E dated August 7, 1989, are provided in Enclosure 1. The response to Action Item 8 references a nonlinear time history analyses report for the Diablo Canyon turbine building; this report is included as Enclosure 2 to this letter.

Action Items 6 and 9-12 are related to the Long Term Seismic Program probabilistic risk assessment and will be the subject of separate correspondence scheduled for submittal in the near future.

Kindly acknowledge receipt of this material on the enclosed copy of this letter and return it in the enclosed addressed envelope.

Sincerely,

J. D. Shiffer

cc: M. P. Bohn (SNL)
R. Fitzpatrick (BNL)
J. J. Johnson (EQE)
J. B. Martin
M. M. Mendonca
P. P. Narbut
B. Norton
M. K. Ravindra (EQE)
H. Rood
B. H. Vogler
CPUC
Diablo Distribution (w/o enc.)

Enclosures

2890S/0072K/DWO/1587



0031
1/1

ENCLOSURE 1

RESPONSE TO ACTION ITEMS FROM THE
LONG TERM SEISMIC PROGRAM
FRAGILITY MEETING, JUNE 16-17, 1989

TABLE OF CONTENTS

**ITEM 1**

The calculations for the RHR heat exchanger did not include a description of how the frequency of the heat exchanger was estimated in the fragility calculation. This frequency based on the pinned-pinned condition is 11.9 Hz, rather than 29.6 Hz as was estimated in design for the condition of three supports. The information on frequency calculations is needed to complete our review.

RESPONSE:

The fundamental frequency of the RHR Heat Exchanger as analyzed by Westinghouse was 29.6 Hz for the horizontal directions. For this case, the anchor bolts act as a moment resisting connection and the intermediate support is active. However, at accelerations approaching failure of the heat exchanger supports, the system softens substantially due to failure of the intermediate support and yield of the anchor bolts. Therefore, the horizontal frequency near the failure level was evaluated by modeling the heat exchanger as a beam with the lower support treated as a pinned connection, the intermediate support not included, and the upper support treated as a pinned connection. This resulted in a pinned-pinned-free two span beam model.

For the RHR heat exchanger, the outside diameter of the shell is 36 inches and the shell thickness is 0.25 inches, which gives a moment of inertia of the cross section of 4486 $in^4$. The total flooded weight is 35,000 lb. The overall height is 339.5 inches, with a distance of 290 inches between the lower support and the upper support which leaves a cantilever span of 49.5 inches above the upper support. From Reference 1, the fundamental frequency of this system is given by the expression

$$f_1 = \frac{\lambda_1^2}{2\pi L^2}\left(\frac{EI}{m}\right)^{1/2}$$

in which $\lambda_1$ depends on the dimensions of the spans and m is the mass per unit length. From the notation in Reference 1, a = 290 in., L = 339.5 in.

$$\frac{a}{L} = \frac{290}{339.5} = 0.854$$

$$m = \frac{35000}{(339.5)(386.4)} = 0.2668 \quad lb-\sec^2/inch^2$$

For the a/L ratio, Reference 1 gives $\lambda_1$ as 3.6. Thus, the fundamental frequency is

$$f_1 = \frac{(3.6)^2}{2\pi(339.5)^2}\left[\frac{(29\times10^6)(4486)}{0.2668}\right]^{1/2} = 12.49Hz$$

In the fragility analysis, a horizontal frequency of 12 Hz was used.

REFERENCES FOR ITEM 1

1. Blevins, R., Formulas for Natural Frequency and Mode Shape, Van Nostrand Rheinhold Co., 1979.

ITEM 2

The nozzle loads on the RHR heat exchanger were scaled from those obtained using Hosgri floor spectra to the median floor spectra at the piping frequency of 12 Hz. Provide a justification for the piping frequency of 12 Hz.

RESPONSE:

The following table summarizes the lowest modal frequencies of the piping runs attached to the RHR Heat Exchangers for which a significant percentage of the piping mass (e.g., > 10%) participates. Thus, these constitute the lowest possible modes which could have contributed significantly to the nozzle loads at the heat exchangers. In all likelihood, higher modes with greater piping mass participation could have been greater contributors. The lowest significant modes are identified for each direction of response for each of the four RHR Heat Exchangers at Diablo Canyon. The frequencies for all directions range from 6.1 to 23.7 Hz with 2/3 of the values greater than 10.5 Hz. The median frequency for all directions and all four heat exchangers is 12.3 Hz. Considering the horizontal and vertical directions separately, the median horizontal frequency is 11.0 Hz, while the median vertical frequency is 18.0 Hz. Considering only RHR Heat Exchanger 1-1, which exhibits the highest Hosgri nozzle loads (the ones factored in the fragility evaluation), the median horizontal and vertical piping frequencies are 11.2 and 17.4 Hz, respectively.

The nozzle loads for the RHR 1-1 Heat Exchanger resulted in support loads which enveloped the loads for the other RHR Heat Exchangers for the Hosgri event. In an attempt to establish the nozzle loads for the reference event, an average horizontal frequency and an average vertical frequency was selected in order to establish a single scaling factor for each directional force and moment. A frequency of 12 Hz was selected for the horizontal direction and a frequency of 25 Hz was selected for the vertical direction. It is noted that these are consistent with the above averages.

For horizontal frequencies less than about 10.5 Hz, the median spectra exceeds the Hosgri spectra, while for frequencies between about 12.5 and 20 Hz, the median spectra

are less than the Hosgri spectra. Thus, the selection of a 12 Hz horizontal frequency constitutes a reasonable value for estimating the Reference event nozzle loads for the RHR Heat Exchangers as a group.

Similarly, at a vertical frequency of 25 Hz, the median vertical ground spectrum exceeds the Hosgri spectrum by the maximum factor of 2.1. In addition, the variability associated with the vertical ground spectrum is nearly maximum at 25 Hz. Thus, the anchor bolt and upper support forces and moments due to piping response from the vertical excitation are somewhat overstated.

Since the nozzle load contribution to the strut loads and anchor bolt shears constitutes only about 25% of the total seismic loads (i.e., inertia of the heat exchanger = 75%) and since the RHR Heat Exchanger has relatively high median and HCLPF capacities and was found not to be a significant contributor to the plant risk, it was judged that a more precise determination of the loads from each nozzle or for each heat exchanger was not warranted for evaluating the RHR Heat Exchangers as a group with a single fragility description.

## Frequencies of Piping Attached to RHR Heat Exchangers

| | | Nozzles | | | |
|---|---|---|---|---|---|
| HX Number | Direction | N1 (Tube-In) | N2 (Tube-Out) | N3 (Shell-In) | N4 (Shell-Out) |
| 1-1 | x | 18.4 | 11.7 | 20.2 | 8.3 |
| | y | 15.4 | 10.5 | 10.6 | 9.2 |
| | z | 23.7 | 8.1 | 16.8 | 18.0 |
| 1-2 | x | 17.8 | 7.9 | 19.4 | 6.8 |
| | y | 14.1 | 11.0 | 14.6 | 7.7 |
| | z | 20.9 | 19.2 | 18.8 | 8.7 |
| 2-1 | x | 8.9 | 9.7 | 18.5 | 13.3 |
| | y | 12.3 | 6.7 | 18.5 | 13.3 |
| | z | 13.7 | 18.4 | 20.5 | 18.1 |
| 2-2 | x | 12.3 | 8.5 | 9.6 | 6.1 |
| | y | 6.7 | 9.6 | 12.2 | 10.9 |
| | z | 10.8 | 18.5 | 8.6 | 13.4 |

All frequencies in Hz

x = North-South
y = East-West
z = Vertical

## ITEM 3

Provide a written summary justifying the factors of 1.2 and 1.5 which were applied to the Test Response Spectra values to obtain fragility values.

RESPONSE:

Recent research has been conducted to establish a reasonable seismic fragility level for components qualified by dynamic testing (References 1 and 2). Since much of the "high level qualification data" (Reference 2) was obtained for Diablo Canyon specific components, a comparison of the results from the research program to assumptions made for the SPRA fragility evaluation was made. In Appendix A, the paper by Dr. Robert P. Kennedy summarizes this comparison showing that the use of the 1.2 and 1.5 factors produce conservative estimates of average spectral acceleration capacity, $\overline{S}_a$ and reasonable estimates of HCLPF $\overline{S}_a$ when combined with the selected variability values used.

REFERENCES FOR ITEM 3


1. Holman, G.S. and C.K. Chou, **Component Fragility Research Program--Phase I Component Prioritization**, NUREG/CR-4899, Lawrence Livermore National Laboratory, Prepared for U.S. Nuclear Regulatory Commission, June, 1987.

2. Tsai, N.C., G.L. Mochizuki, and G.S. Holman, **Component Fragility Research Program--Phase II Development of Seismic Fragilities from High Level Qualification Data** (draft), Lawrence Livermore National Laboratory, Prepared for U.S. Nuclear Regulatory Commission, June, 1989.

**ITEM 4**

Provide and discuss the basis for the seal leakage assumptions and the failure mode used in the reactor coolant pump fragility calculations.

RESPONSE:

The potential failure modes of the Reactor Coolant Pump include the loss of function and structural failure modes leading to Loss of Coolant Accidents. The most critical of the functional failure modes is the result of the loss of offsite power. Since the loss of offsite power occurs at low acceleration levels, other functional failure modes that are related to earthquake induced stresses and deformations are estimated to occur at much higher acceleration levels and are not considered. The most critical of the structural failure modes involves the loss of seal capability due to excessive deformation of the lower motor stand. Comparing the overall impact of these failure modes, note that the loss of power only renders the pump inoperable without a LOCA, while the structural failure mode results in a small or seal LOCA. Thus, the fragility of Reactor Coolant Pump is based on the excessive bending failure of the lower motor stand.

The identification of this structural failure mode is based on discussions with Westinghouse personnel. Information obtained from Westinghouse indicated that the RCP has three seals. The first is located about 3 inches below the lower motor stand flange, while the third is located about 18 inches above the lower motor stand flange. Westinghouse also indicated that in order to affect seal leakage, the pump shaft must be excessively disturbed in the vertical direction. In addition, in the event that the lower motor stand should bend inelastically, the shaft, having a low flexural stiffness compared to the lower motor stand, would follow the motor and bend about the seal housing.

Noting that the pump shaft must be significantly displaced in the vertical direction, it is not likely that the vertical earthquake motion would be sufficient to cause seal leakage. The RCP is relatively stiff in the vertical direction, having a vertical frequency of 21 Hz. The vertical mode is governed primarily by the deformation of the main support below the lower

motor stand. Therefore, little vertical amplification is expected in the pump and it is judged that the vertical response does not produce displacements sufficiently large to drive this failure mode.

Vertical displacements of the pump shaft large enough to lead to seal leakage can only be obtained through compatibility with excessive horizontal displacements of the motor. In order to develop such large horizontal displacements, it is judged that the formation of a plastic hinge in the lower motor stand is necessary. With the development of the plastic hinge, the inelastic flexural deformations cause the center of gravity of the motor to translate horizontally while also rotating downward. The lower motor stand is the expected location for the plastic hinge since it has a reduced cross-section due to the two cut-out portions and is the flexural weak link of the RCP. The formation of the plastic hinge is driven by the horizontal response, which controls the earthquake stresses based on the relative amplitudes of the reference floor spectral accelerations ($S_{a\,NS} = 3.04g$, $S_{a\,EV} = 2.87g$, and $S_{a\,V} = 1.57g$).

**ITEM 5**

Provide, in tabular form, the basis for each of the various beta values identified in Enclosure 3 to this meeting summary.

The following responses are included to answer the questions as it was asked in the formal request. However, during the NRC fragility evaluation review meetings, it was requested that a more detailed discussion of the determination of randomness and uncertainty variability be included giving examples for a couple of equipment components and qualification methods. To provide this additional insight, a discussion of the bases for the variabilities for the Reactor Coolant Pump (structural failure mode) and the Diesel Generator Control Panel (functional and structural failure modes) are included as an attachment in Appendix B.

All of the page references in the questions in this item pertain to Reference 1.

QUESTION 1 - reference to Page 5-27

The equipment frequency variation is represented by a logarithmic standard deviation, $\beta$, ranging from 0.09 to 0.20. Provide the bases of this estimation.

RESPONSE:

The equipment frequency variability is included to account for variation in the natural frequency as determined by analysis or test. Since the $\beta$ value applied in the fragility evaluation depends on the complexity and boundary conditions of the specific equipment under consideration, the logarithmic standard deviation was taken to range from 0.09 to 0.20. This range was based on the results of Reference 2 as well as judgment considering the various equipment types and the expected ability of an analyst or a test laboratory to adequately represent the true component. As discussed in Reference 1, the sources of the variability include the ability of an analytical model to properly capture the in-situ boundary conditions and the adequacy of the attachment to a shake table in matching the actual plant installation.

Since the boundary conditions are the greatest contributor to the uncertainty, a component having a frequency uncertainty at the low end of the range would be a simple component whose frequency was established by test or by detailed analysis and is anchored to the floor by welds to embedded plates or bolted with known specified bolt torques. For a component with $\beta_f = 0.09$, the 5% - 95% confidence range about the median frequency is approximately ± 15%. On the other hand, for a complex component whose frequency was established by approximate methods or, if qualified by test, has an in-situ anchorage which is different than that used in the test, a higher frequency uncertainty is recommended. For such cases, with $\beta_f = 0.20$, the 5% - 95% confidence range about the median frequency is approximately ± 40%.

QUESTION 2 - reference to Page 5-28
An uncertainty variability on equipment mode shape is assumed to range from 0.05 to 0.15. Provide the basis of this estimation.

RESPONSE:

The equipment mode shape uncertainty represents the contribution to the response variability due to modeling errors in capturing the proper mode shape of the component. The magnitude of the β value depends on the complexity of the component. Reference 2 utilized a mode shape variability of 0.15 for multi-degree-of-freedom systems, which was based on the authors' experience in conducting many dynamic analyses. For equipment components that can be adequately represented with very simple dynamic models (e.g., single degree of freedom models), a much lesser mode shape variability could be used. Thus, the equipment mode shape uncertainty ranging from 0.05 to 0.15 is judged to be appropriate.

QUESTION 3 - reference to Page 5-42

Explain how $\beta_R = 0.17$ and $\beta_U = 0.10$ were obtained for high frequency components located on floor levels at or above the C.G. of the structure.

RESPONSE:

In response to seismic input, as a structure begins to yield and behave inelastically, the observed response frequency tends to shift from the elastic frequency to lower frequencies as the system softens. An outcome of this is that the inelastic spectral accelerations tend to reduce relative to the scaled elastic spectra at frequencies near the peak of the floor spectra. However, it has been observed that, at higher frequencies, the inelastic floor spectral accelerations can show an increase over those predicted by the elastic spectra. Whether the inelastic spectral accelerations are higher or lower than the scaled linear spectra depends on the dynamic characteristics of the structure and the frequency content of the earthquake ground motion. Thus, this variability has contributions from both randomness and uncertainty.

To include this effect for high frequency components, a composite variability, $\beta_C$ of 0.20 was taken to represent the variability due to the inelastic structure response at or above the center of gravity of the structure. This value for $\beta_C$ was based on the results of a study addressing the effects of ground motion characteristics on structural response (Reference 4). It was also found in Reference 4 that the frequency content of the ground motion was the most substantial factor contributing to this effect. This could be expected since, due to the effective frequency shift, the relative amplitudes of the spectral accelerations on the soft (lower) frequency side of the elastic frequency and at the elastic frequency strongly influence the amplitude of the inelastic response. Therefore, a higher variability was assigned to randomness than to uncertainty. From the composite variability of 0.20, the randomness and uncertainty variabilities were then judged to be $\beta_{IR_R} = 0.17$ and $\beta_{IR_U} = 0.10$.

QUESTION 4 - reference to Page 5-49

Justify the assumption that spectra corresponding to 1.2 times the median spectra represents a 95% confidence upper bound. Why not 1.1 or 1.25, etc?

RESPONSE:

To establish the median seismic stresses in the motor stand, the median floor spectra at El 114 ft had to be estimated, since the median spectra were only generated at El 140 and 85 ft. The median spectra at El 114 ft were interpolated from the 140 and 85 ft spectra using the relative Hosgri spectral accelerations. The interpolation was based on the judgment that the general shape of the floor spectra for the Hosgri and reference ground motion should be the same although the peak frequencies are different. It was held that the ratio of the median spectra to the Hosgri spectra at their respective peak frequencies should be similar at all elevations or at least exhibit a trend that could be interpolated. This same expectation was held for the frequencies when expressed as a ratio of the peak frequencies. To estimate the uncertainty associated with the interpolation, it was judged that an increase of 20%, i.e. scaling by 1.2, in the interpolated spectral accelerations represented a 95% confidence upper bound. This was felt to be a reasonable estimate since the interpolation included the relative spectral accelerations as well as the relative amplification with respect to the peak frequencies. Therefore, the uncertainty associated with the estimated spectral accelerations used to calculate the median seismic stresses was evaluated as

$$\beta_{US_a} = \frac{1}{1.65}\ln(1.20/1.00) = 0.11$$

QUESTION 5 - reference to Page 5-50

Provide the basis that assuming plastic hinge formation at 90% of the full plastic section would represent a 95% confidence lower bound.

RESPONSE:

The development of the failure mode is dependent on attaining large horizontal displacements resulting from the formation of a plastic hinge in the cut-out portion of the lower motor stand. In order to develop the displacements, a large amount of plastic deformation is required beyond that at which the hinge first forms. Further, the plastic hinge does not form until the complete section is stressed to yield. However, there is the possibility that, due to slight geometric irregularities, the plastic hinge could develop at a slightly reduced moment below the theoretical plastic moment. The shape factor for the cut-out section (the ratio of the plastic to elastic section modulus) was calculated to be 1.46, which indicates that there is substantial margin between the development of first yield in the section and the formation of a plastic hinge. Because the cut-out section of the lower motor stand has such capacity beyond initial yield, it is expected that the plastic hinge mechanism does not develop until the section becomes fully plastic or very nearly fully plastic such that the required horizontal displacements could be attained. In addition, since the cross section is essentially circular, the variability is expected to be low. Therefore, it was judged that a 95% confidence lower bound for the formation of the plastic hinge could be represented as the point at which the section was 90% fully plastic. Therefore,

$$\beta_{UP} = \frac{1}{-1.65} \ln(0.90/1.00) = 0.06$$

QUESTION 6 - reference to Page-5-54

Variability on equipment frequency is expressed as a $\beta_U$ of 0.085 to 0.20. This is different from 0.09 to 0.20 as stated in Section 5.1.1.2 (reference to item 1). Explain the reason.

RESPONSE:

The stated range of the equipment frequency variability is different than the range of 0.09 to 0.20 as stated in Section 5.1.1.2 and as discussed in the response to Question 1 of this Item. This is merely an inconsistency in the text of the report as they are not intended to be different for a specific reason. This difference has no bearing on the fragility results contained in the report.

QUESTION 7 - reference to Page 5-55

Why consider a $\pm 1\,\beta$ relative frequency shift? How was the frequency range 5.6 to 8.5 Hz, calculated?

RESPONSE:

The variability due to frequency has contributions from both the equipment frequency and the structure frequency, with the equipment frequency typically having a variability ranging from 0.09 to 0.20. The $\beta_U$ for the reactor coolant pump was taken to be 0.15 and the uncertainty associated with frequency of the Containment building internal structure was taken as 0.15. Therefore, the overall frequency uncertainty was estimated as

$$\beta_{fU} = (0.15^2 + 0.15^2)^{1/2} = 0.21$$

The frequency variability alone does not measure the impact of the modeling error. It is necessary to relate this variability to a response quantity in order to measure the impact of the frequency modeling error. Depending on the shape of the response spectrum, a shift in the natural frequency can have a dramatic effect or no effect at all. For example, if the median frequency is on a steep slope of the response spectrum, a $\pm 1\beta$ frequency shift can cause a significant increase in the spectral acceleration. However, if the median frequency is on a flat portion of the spectrum, the frequency shift can have no effect at all. Generally, the $\pm 1\beta$ variation in modeling uncertainty due to frequency error is taken as the variation in response over the $\pm 1\beta$ frequency range.

With the median fundamental frequency of the reactor coolant pump having a value of 6.9 Hz, the $\pm 1\beta$ frequency values are evaluated as

$$f_{-1\beta} = 6.9e^{-0.21} = 5.6Hz$$

$$f_{1\beta} = 6.9e^{0.21} = 8.5Hz$$

The median frequency falls on the low frequency side of the horizontal floor spectra, which peak at a frequency of about 8 Hz for both the NS and EW directions. By considering a $\pm 1\beta$ frequency shift about the median, the global maximum horizontal spectral accelerations are included in the frequency range. Since the global maxima of the response spectra are contained within the $\pm 1\beta$ frequency range, the response variation represents a wider variation than just $\pm 1\beta$. From 5.6 to 8.5 Hz, the median horizontal spectral floor acceleration vector is 3.36g and the maximum vector is 4.28g. These vector magnitudes were calculated from the orthogonal horizontal components with 100% of the NS spectral acceleration and 40% EW spectral accelerations. In the evaluation of the Strength Factor, the directional responses were combined using the median centered 100/40/40 method. The Strength Factor was based on an acceleration vector of 3.25g at 6.9 Hz. Therefore, the Modeling Factor associated with frequency was evaluated as 3.25/3.36 = 0.97. The modeling uncertainty associated with frequency was estimated by considering the maximum horizontal spectral acceleration vector in the $\pm 1\beta$ frequency range to be a $2.33\beta$ upper bound (99% confidence bound), since the $\pm 1\beta$ frequency interval included the global maxima of the floor spectra. The modeling uncertainty associated with frequency then becomes

$$\beta_{fu} = \frac{1}{2.33}\ln\left(\frac{4.28}{3.36}\right) = 0.10$$

QUESTION 8 - reference to Page 5-59

Justify $\beta_{IRC} = 0.10$. Also explain the calculation of $\beta_{IRR}$ and $\beta_{IRU}$.

RESPONSE:

As a structure responds inelastically, the spectral accelerations tend to decrease at frequencies near the peak of the floor spectra. However, this is not always true at higher frequencies. At high frequencies, the inelastic spectral accelerations can show an increase over those predicted from linear spectra. Whether the inelastic spectral accelerations are higher or lower than the scaled linear spectra depends on the dynamic characteristics of the structure and the frequency content of the earthquake ground motion. To account for the possibility of higher inelastic spectral accelerations, a composite variability, $\beta_C$, of 0.20 was taken to represent the variability due the inelastic structure response at or above the C.G. of the structure. This value for $\beta_C$ was based on the results of Reference 4. The randomness and uncertainty variabilities were separated from the composite value as $\beta_{IRR} = 0.17$ and $\beta_{IRU} = 0.10$.

While the variabilities described above are applicable to high frequency components, they are not directly applicable to the reactor coolant pump. The median fundamental frequency of the RCP has a value of 6.9 Hz, which lies on the soft (low frequency) side of the peak of the floor spectra. As the structure responds into the inelastic range, there will be an apparent shift to lower frequencies. However, based on the elastic spectra, a shift to lower frequencies would tend to produce lower spectral accelerations. As a result, it is less likely that the inelastic spectral accelerations will exceed the scaled elastic spectra in this lower frequency range. Therefore, a lower value of $\beta_C$ equal to 0.10 was used to account for the variability in the inelastic spectra at or above the vertical C.G. of the structure. The randomness and uncertainty variabilities were separated from the composite variability in the same proportions as for the high frequency case, with $\beta_{IRR} = 0.085$ and $\beta_{IRU} = 0.05$.

The above values correspond to locations at or above the center of gravity of the structure. However, at the basemat level, variabilities are taken to be zero. Since the RCP is located at El 114 ft which is between the basemat at El 85 ft and the C.G. at El 140 ft, the variabilities of the Inelastic Structural Response Factor are interpolated as

$$\beta_{IR_R} = \left(\frac{114-85}{140-85}\right)(0.085) = 0.05$$

$$\beta_{IR_U} = \left(\frac{114-85}{140-85}\right)(0.05) = 0.03$$

QUESTION 9 - reference to Page 5-84
Explain the calculation of $\beta_{ECC_R}$ and $\beta_{ECC_U}$.

RESPONSE:

The randomness and uncertainty variabilities were evaluated using estimated relative response contributions from each of the three earthquake component directions. The randomness, $\beta_{ECC_R}$, represents variability due to the random phasing of the three components. An SRSS combination of the directional contributions is judged to be median centered, while an absolute sum of the three components represents a worst case upper bound or equivalently, a +3 $\beta$ upper bound. The randomness variability was evaluated by considering a support in which all three earthquake directions significantly contribute to the overall loading with one direction dominating. Using relative response contributions $R_X = 1.0$, $R_Y = 0.5$, and $R_Z = 0.5$, $\beta_{ECC_R}$ was evaluated as

$$\beta_{ECC_R} = -\frac{1}{3}\ln\left(\frac{[R_x^2 + R_y^2 + R_z^2]^{1/2}}{R_x + R_y + R_z}\right)$$

$$= -\frac{1}{3}\ln\left(\frac{[1.0^2 + 0.5^2 + 0.5^2]^{1/2}}{1.0 + 0.5 + 0.5}\right) = 0.16$$

The uncertainty in $F_{ECC}$ comes from the variability in the relative contributions of the earthquake components for the various pipe supports. The pipe supports were designed using the absolute sum of the worst horizontal plus the vertical input. This directional

combination method can be either conservative or unconservative compared to the median centered SRSS method, depending on the relative loadings from each of the earthquake directions. To illustrate this, consider the extreme conservative and unconservative cases.

First, consider the unconservative condition in which the two horizontal components have equal contributions to the overall load, while the vertical direction has no contribution, i.e., $R_{H1} = 1.0$, $R_{H2} = 1.0$, and $R_V = 0.0$. Comparing the combined responses from the worst horizontal plus vertical method with the SRSS method gives

$$H + V: \; R_{H1} + R_V = 1.0 + 0.0 = 1.0$$

$$SRSS: \; (R_{H1}^2 + R_{H2}^2 + R_V^2)^{1/2} = (1.0^2 + 1.0^2 + 0.0^2)^{1/2} = 1.414$$

Taking the ratio of the two

$$\frac{H+V}{SRSS} = \frac{1.0}{1.414} = 0.707$$

This shows that, in the most unconservative situation, the worst horizontal plus vertical method is unconservative by a factor of 1.4.

Next, consider the most conservative condition where the overall load has equal contributions from only one horizontal component and the vertical component, i.e., $R_{H1} = 1.0$, $R_{H2} = 0.0$, and $R_V = 1.0$. Comparing the two combination methods,

$$H + V: \; R_{H1} + R_V = 1.0 + 1.0 = 2.0$$

$$SRSS: \; (R_{H1}^2 + R_{H2}^2 + R_V^2)^{1/2} = (1.0^2 + 0.0^2 + 1.0^2)^{1/2} = 1.414$$

Taking the ratio of the two,

$$\frac{H+V}{SRSS} = \frac{2.0}{1.414} = 1.414$$

In this most conservative case, the worst horizontal plus vertical method is conservative by a factor of 1.4.

The uncertainty, $\beta_{ECC_U}$, was evaluated by considering these two extreme cases to be the $\pm 3\beta$ bounds for the possible loading condition on the pipe supports due the three earthquake component directions. Therefore, the variation from the most unconservative to the most conservative conditions represents a 6 standard deviation range. Thus,

$$\beta_{ECC_U} = \frac{1}{6} \ln\left(\frac{1.414}{0.707}\right) = 0.12$$

REFERENCES FOR ITEM 5


1. Kipp, T.R., Wesley, D.A., Nakaki, D.K., and Kennedy, R.P., **Seismic Fragilities of Civil Structures and Equipment Components at the Diablo Canyon Power Plant,** NTS Engineering Report No. 1643.02, Revision 0, January, 1989.

2. Kennedy, R.P., et. al., **Subsystem Response Review, Seismic Safety Margins Research Program,** NUREG/CR-1706, July, 1981

3. Kennedy, R.P., et. al., **Subsystem Fragility, Seismic Safety Margins Research Program (Phase I),** NUREG/CR-2405, February, 1982.

4. Kennedy, R.P., et. al., **Engineering Characterization of Ground Motion, Task II ,** NUREG/CR-3805, Vol. 2, March, 1985.

**ITEM 7**

In many instances, relays were seismically qualified by testing a component assembly, such as a cabinet containing a number of relays. Discuss how PG&E computed the fragilities of such assemblies when some of the relays have been replaced, and whether or not requalification tests were used.

RESPONSE:

An extensive program was conducted by PG&E to identify critical relays. The objectives of the investigation were to identify relays that affect components necessary for safe shutdown, to identify the relays associated with those components that are potentially subject to seismic induced chatter, to determine the consequences of the chatter, and to determine the required corrective actions. As a result, those relays subject to chatter and having negative consequences were identified. The location and the orientation of the contact positions were also determined.

The functional failure fragilities of relays were evaluated only for those relays identified by PG&E as being chatter sensitive. The identified relays are installed in their respective component assemblies in the plant consistent with the qualification tests which formed the basis for the functional fragilities. The method for evaluating the Strength factor for functional failures is given in Reference 1 as

$$F_s = \frac{1.15 \times GERS}{A_q \times S_a}$$

in which GERS is the Generic Equipment Ruggedness Spectrum taken from Reference 2, $A_q$ is the acceleration amplification factor of the cabinet for the critical direction which is based on transmissibility data from qualification tests or generic tests, and $S_a$ is the floor spectral acceleration.

The replacement of relays in a cabinet does not impact the reported fragilities so long as the new relays are the same model with the same orientation and critical direction. If some relays are replaced with like models, requalification testing is not needed since the fragilities are based on the GERS for the specific model relays.

For those cases where a relay is replaced by a commercial grade or other non-identical component or where a component is added to a previously tested cabinet, PG&E procedures (Reference 3) contain requirements for testing and analysis to assure that the new or added component is qualified for the in-cabinet seismic environment and that the presence of the new or added item does not compromise the qualification of the other safety related components within the cabinet.

REFERENCES FOR ITEM 7


1. Kipp, T.R., Wesley, D.A., Nakaki, D.K., and Kennedy, R.P., **Seismic Fragilities of Civil Structures and Equipment Components at the Diablo Canyon Power Plant**, NTS Engineering Report No. 1643.02, Revision 0, January, 1989.

2. Smith, C.B. and Merz, K.L., **Generic Seismic Ruggedness of Power Plant Equipment**, EPRI Report NP-5223, ANCO Engineers, Inc., May, 1987.

3. PG&E Nuclear Engineering Procedures Manual, Procedure No. 3.12, "Spare and Replacement Parts Evaluation."

**ITEM 8**

Discuss the impact on the turbine building nonlinear analysis of closure of the gap between the turbine pedestal and the floor at Wall 31 in the turbine building.

RESPONSE:

The results of multiple nonlinear time history analyses which were conducted to study drifts and probabilities of failure of Walls 19 and 31 of the Diablo Canyon Turbine Building have been presented in References 1 and 2. These analyses were based upon the analytical model shown in Figures 2-2 and 2-3 of Reference 1. This model is predicated on the assumption that the most likely location of impact between the operating floor and turbine pedestal is at the center of the operating floor span. This assumption is valid for the vast majority of the trial cases in which the center of the operating floor deforms substantially more than the turbine pedestal and drifts into the turbine pedestal which arrests further drift of the operating floor. However, for a few of the trial cases, the turbine pedestal drift is sufficiently large that the turbine pedestal is likely to impact the operating floor near the edges of the turbine pedestal adjacent to Walls 19 and 31. This potential problem is particularly severe near Wall 31 because the edge of the turbine pedestal is immediately adjacent to Wall 31. In these cases, impact of the turbine pedestal into the operating floor could result in forcing the drift of the top of Wall 31 (Elev. 140) to be greater than that reported in References 1 and 2 using the analytical model shown in Reference 1, which in turn, could increase the probability of failure of the Turbine Building above the reported levels. A conservative bounding evaluation of this possibility is presented herein.

If one conservatively assumes that impact of the turbine pedestal into the operating floor immediately adjacent to the stiff Wall 31 does not reduce the turbine pedestal drifts below those computed from the model of Reference 1, which assumes impact at the center of the operating floor, then the drift of Elev. 140 of Wall 31 due to this edge impact can be estimated from:

$$\delta_{Top31} = \delta_{TP} - Gap \qquad (1)$$

where $\delta_{TP}$ is the computed turbine pedestal drift using the model of Reference 1, and Gap is the gap size. Actual gap sizes adjacent to Wall 31 are estimated to average between 3.75 and 4.25 inches. Instead, a conservative gap size of 3.375 inches will be used. Thus:

$$\delta_{Top31} = \delta_{TP} - 3.375 \quad \text{inches} \tag{2}$$

It is expected that Equation (2) conservatively overestimates the drift at the top of Wall 31 due to edge impacts because:

(1) $\delta_{TP}$ ignores the influence of the immediately adjacent stiffness of Wall 31 which is large.

(2) 3.375 inches is an underestimate of the gap size.

Whenever $\delta_{Top31}$ computed from Equation (2) exceeds the drift computed for the top of Wall 31 in the analyses of References 1 and 2, the possibility exists that this edge impact could increase the probability of failure of Wall 31. This situation never occurs for any of the cases which used median structural models (randomness only), as can be observed from Table 1 of Reference 2 ($\overline{S}_A = 2.25g$) and Tables 5-1 ($S_A = 3.0g$) and 5-2 ($\overline{S}_A = 6.0g$) of Reference 1. Thus, the reported probabilities of failure for the Randomness Only Cases is not influenced by the possibility of an edge impact.

However, for a small fraction of the trials with uncertain structural properties, the top drift computed for Wall 31 from Equation (2) exceeds that obtained using the analytical model of Reference 1. All of these trials are listed in Table 1. They consist of 3 trials at $\overline{S}_A = 2.25g$, 7 trials at $\overline{S}_A = 3.0g$, and 10 trials at $\overline{S}_A = 4.0g$ and 6.0g out of 50 trials at each ground motion level. The Reference drifts and probabilities of failures are those developed from the analytical model of Reference 1.

The top drift from Equation (2) is a relative displacement induced drift; as such, it will be spread nearly uniformly over the full 55-foot wall height, rather than being concentrated into the lowest story of Wall 31 as are the inertially induced drifts obtained for the Reference case using the analytical model of Reference 1. Thus, this Equation (2) drift should be compared with a drift criterion expressed in terms of total wall height (55 feet) rather than story height.

The probability of failure versus shear wall drift criteria presented in Equation 2-5 of Reference 1 is intended for application per story height and might be too liberal when applied to an average drift over the full wall height. Based upon the same shear wall severe distress versus drift data described in Section 2.1.3 of Reference 1 and the Response to Question 29 in Reference 3, the following more conservative drift criterion, which is judged to be appropriate for application over the total wall height (55 feet), was chosen:

Median Drift Limit, D = 0.6%

(3)

Composite Variability, $\beta_c = 0.285$

This criterion leads to the following Probability of Severe Distress versus the Equation (2) drifts:

| Equation (2) Drift (inches) | Probability of Severe Distress $P_P$ (%) |
|---|---|
| 1.65 | 0 |
| 2.48 | 5 |
| 2.98 | 16 |
| 3.96 | 50 |
| 5.26 | 84 |
| 6.33 | 95 |
| 9.50 | 100 |

The resulting revised $P_F$ is reported in Table 1 for every trial where the Equation (2) drift, coupled with the Equation (3) failure criterion, leads to a higher computed probability of failure than was originally reported in References 1 and 2. As shown in Table 1, this condition exists for only one trial at $\overline{S}_A = 2.25g$, 3 trials at $\overline{S}_A = 3.0g$, and 4 trials at $\overline{S}_A = 4.0g$ and 6.0g out of 50 trials at each ground motion level. Furthermore, the increase is only significant at one trial each at $S_A = 3.0$, 4.0, and 6.0g. Table 1 also presents the revised $\Sigma P_F$ for all 50 trials using these revised increased individual $P_F$ accounting for pedestal impact adjacent to Wall 31. These revised $\Sigma P_F$ estimates lead to the following revised estimates of the overall composite (randomness plus uncertainty) $P_F$ estimates versus ground motion level:

| $\bar{S}_A(g)$ | Revised Composite $P_F$ (%) | Reference Composite $P_F$ (%) | Reference Lognormal Fragility Estimate PF (%) |
|---|---|---|---|
| 2.25 | 3.0 | 2.9 | 2.7 |
| 3.0 | 11.5 | 11.1 | 12.5 |
| 4.0 | 38.2 | 37.2 | 35.5 |
| 6.0 | 77.9 | 76.7 | 76.5 |

The Reference Lognormal Fragility Estimate of Equation 6-1 of Reference 1, which was based upon the computed Reference Composite $P_F$ from Reference 1, fits very well with these Revised Composite $P_F$ results. If the Equation 6-1 of Reference 1 lognormal fragility estimate had been based upon these Revised Composite $P_F$ results, the Median $S_A$ could have been 4.55g versus the reported value of 4.59g, with all of the variabilities remaining unchanged. Thus, throughout the entire probability range, the reduction in capacity would be only 1%, which is totally trivial considering the underlying uncertainties and considering that the Revised Composite $P_F$ is based upon the following conservative assumptions:

(1) Potential reduction in the turbine pedestal drift due to impact immediately adjacent to the stiff Wall 31 is ignored.

(2) The gap size is conservatively underestimated.

(3) The probability of severe distress versus drift criterion of Equation (3) is likely to be conservative.

REFERENCES FOR ITEM 8


1. Kennedy, R. P., D. A. Wesley, and W. H. Tong, **Probabilistic Evaluation of the Diablo Canyon Turbine Building Seismic Capacity Using Nonlinear Time-History Analyses**, No. 1643-01, NTS Engineering, December 1988.

2. Kennedy, R. P., M. W. Salmon, and D. K. Nakaki, **Additional Nonlinear Time-History Analyses for Diablo Canyon Turbine Building**, No. 11-0170-0031, Impell Corporation, May 1989.

3. **Diablo Canyon Long-Term Seismic Program--Docket Nos. 50-275 and 50-323**, Pacific Gas & Electric Company, January 1989.

Table 1: Nonlinear Drifts at Top of Wall 31

| Trial | $\overline{S}_A = 2.25g$ | | | | $\overline{S}_A = 3.0g$ | | | | $\overline{S}_A = 4.0g$ | | | | $\overline{S}_A = 6.0g$ | | | |
|---|---|---|---|---|---|---|---|---|---|---|---|---|---|---|---|---|
| | Reference | | Equation (2) | | Reference | | Equation (2) | | Reference | | Equation (2) | | Reference | | Equation (2) | |
| | Drift (inch) | PF (%) | Drift (inch) | PF (%) | Drift (inch) | PF (%) | Drift (inch) | PF (%) | Drift (inch) | PF (%) | Drift (inch) | PF (%) | Drift (inch) | PF (%) | Drift (inch) | PF (%) |
| 2 | | | | | | | | | 2.00 | 91.1 | 2.15 | | 5.17 | 99.7 | 6.84 | |
| 15 | 1.37 | 5.5 | 1.78 | | 2.83 | 82.6 | 3.12 | | | | | | | | | |
| 18 | 0.14 | 0 | 0.28 | | 1.20 | 9.3 | 1.44 | | 5.16 | 63.7 | 8.74 | 99.7 | 5.80 | 98.6 | 19.00 | 100.0 |
| 22 | | | | | 1.55 | 18.7 | 1.91 | | 3.08 | 56.8 | 3.81 | | | | | |
| 24 | | | | | | | | | 1.14 | 2.3 | 1.30 | | 2.29 | 72.9 | 2.87 | |
| 27 | | | | | | | | | 1.19 | 4.7 | 1.49 | | 2.48 | 59.9 | 3.97 | |
| 34 | | | | | 0.41 | 0 | 1.56 | | 1.40 | 4.7 | 2.68 | 8.5 | 4.62 | 91.6 | 9.05 | 99.8 |
| 41 | | | | | | | | | | | | | 6.83 | 98.2 | 6.88 | |
| 43 | 0.58 | 0 | 2.40 | 3.9 | 2.14 | 44.8 | 4.36 | 63.2 | 5.16 | 94.6 | 6.91 | 97.5 | 11.65 | 100.0 | 15.42 | |
| 45 | | | | | | | | | 1.46 | 4.0 | 1.61 | | 3.49 | 44.8 | 6.58 | 96.3 |
| 48 | | | | | 1.06 | 2.4 | 2.44 | 4.5 | 2.78 | 63.7 | 2.94 | | 5.08 | 93.1 | 6.24 | 94.5 |
| 49 | | | | | 0.97 | 0.4 | 2.08 | 1.2 | 1.84 | 28.8 | 3.49 | 32.9 | 6.65 | 99.7 | 6.96 | |
| | | | Σ=151.0 | | | | Σ=574.9 | | | | Σ=1907.6 | | | | Σ=3896.3 | |

**ITEM 13**

Provide a written summary of the presentation made at the meeting in response to the hazard/fragility interface question listed in Enclosure 3 to this meeting summary.

RESPONSE:

Essentially all seismic probabilistic risk assessment (SPRA) studies have used a single ground motion parameter as the interface parameter between the seismic hazard prediction and the seismic fragility estimation. Most previous SPRA studies have used the peak ground acceleration (PGA) or effective peak ground acceleration (EPGA) as this interface parameter. However, for the reasons described herein, in the Diablo Canyon LTSP SPRA the average spectral acceleration over the 5 to 14 Hz range ($\overline{S}_A$) was used as the interface parameter. We consider the use of $\overline{S}_A$ as the interface parameter to represent a significant improvement over using PGA or EPGA.

In an SPRA, the spectral acceleration at any given frequency is given by:

$$S_{A(f)} = AF \cdot SAR \qquad (1)$$

where

$$AF_{(f)} = \frac{S_{A(f)}}{SAR}$$

is the transfer factor defined by some median spectrum shape anchored to SAR, and SAR is the chosen interface ground motion parameter (either $\overline{S}_A$, PGA, or some other parameter). Both $AF_{(f)}$ and SAR are random variables whose variability may be estimated from a suite of ground motion records judged appropriate for the site conditions. In essentially all SPRA studies, including Diablo Canyon, for earthquakes at a given magnitude and range, both SAR and $AF_{(f)}$ are considered to be lognormally distributed for which variabilities can be expressed by the logarithmic standard deviations $\beta_{SAR}$ and $\beta_{AF}$, respectively. The variability, $\beta_{SAR}$, is included within the variability estimate for the seismic hazard since it is simply an expression

of the attenuation relationship variability. The variability, $\beta_{AF}$, is included in the random variability for the fragility estimate and is often called the "spectral shape variability" or "peak and valley variability in spectral shape." This standard approach is rigorously equivalent to assuming that for a given magnitude, range, and attenuation relationship, the spectral acceleration, $S_{A(f)}$ at any frequency is lognormally distributed with logarithmic standard deviation:

$$\beta'_{S_A} = [\beta^2_{SAR} + \beta^2_{AF}]^{1/2} \tag{2}$$

However, Equation (2) is only rigorous when SAR and AF are independent random variables. Otherwise, Equation (2) needs to be rewritten as:

$$\beta_{S_A} = [\beta^2_{SAR} + \beta^2_{AF} + CC]^{1/2} \tag{3}$$

where CC represents the cross-correlation term. To the best of our knowledge, every SPRA study has assumed that SAR and AF are independent random variables (i.e., Equation (2)). This assumption is adequate so long as the cross-correlation terms CC are small.

It will be shown that when $\overline{S}_A$ is used as the interface ground motion parameter SAR, throughout the frequency range from 3.3 Hz and greater, $\beta'_{S_A}$ from Equation (2) accurately predicts $\beta_{S_A}$ (i.e., the ignored cross-correlation terms is small). However, when PGA is used for SAR, $\beta'_{S_A}$ from Equation (2) severely overpredicts $S_A$ at frequencies below about 15 Hz (i.e., the ignored cross-correlation term is significantly negative). Ignoring a significant negative CC term will introduce a conservative error into the SPRA.

For use in the Diablo Canyon SPRA, the median $AF_{(f)}$ and its variability $\beta_{AF}$ were developed from 38 pairs of horizontal ground motion records (two horizontal components each) as discussed in Chapter 6 of Reference 1. These 38 pairs came from 12 pairs of empirical time-histories (used twice each with reversed orthogonal axes), and 14 pairs of numerical generated records. Each of the 38 pairs of records was scaled to have the same SAR value (either $\overline{S}_A$ or PGA) for the average of the two horizontal components. From these 38 scaled pairs, the 50% and 84% non-exceedance probability (NEP) transfer factors $AF_{(f)}$ were developed from a number of frequencies ranging from 3 to 30 Hz for the average of the two

horizontal response components. Figures 1 and 2 present the ratio of 84%/50% AF when $\overline{S}_A$ and PGA are used, respectively, as the ground motion interface parameter SAR. As can be seen in Figure 1, when $\overline{S}_A$ is used, the ratio of 84%/50% $A_F$ can be taken to be 1.20 for all frequencies greater than 3.3 Hz, including the zero period acceleration (ZPA) which is plotted at 100 Hz. However, Figure 2 shows that when PGA is used, no reasonable constant value for the ratio of 84%/50% $A_F$ can be chosen for the entire frequency range from 3 to 30 Hz. One might choose a varying ratio ranging from about 1.4 at 3.5 Hz to 1.15 at 30 Hz. Alternatively, one might choose and average ratio of 1.33 from 3.3 to 15 Hz, but this ratio would be excessively conservative above 15 Hz. In the following discussions, we will make the former choice.

If one assumes that $A_F$ is lognormally distributed, then

$$\beta_{AF} = \ln(84\%/50\%) \tag{4}$$

from which the estimates of $\beta_{AF}$ given in Table 1 can be obtained. For multiple frequency components, substantial simplification is achieved in estimating the fragility variabilities when $\beta_{AF}$ is assumed to be frequency-independent (constant). Furthermore, at frequencies below 20 Hz, the variability, $\beta_{AF}$, is less when $\overline{S}_A$ is used as the interface parameter rather than PGA. For both of these reasons, $\overline{S}_A$ is preferable as a choice for the interface parameter over PGA. However, the final choice on the interface parameter should be based on which parameter allows $\beta'_{S_A}$ from Equation (2) to best approximate $\beta_{S_A}$ (i.e., near zero cross-correlation term).

Based on regression analyses perform on a large number of ground motion records, Table 4.5 of Reference 1 shows that for a given magnitude and range, $\beta_{SAR} = 0.36$ irrespective of whether PGA or $\overline{S}_A$ is chosen as the interface parameter SAR. From these same regression analyses, Table 4.5 of Reference 1 also presents $\beta_{S_A}$ for several different frequencies. These $\beta_{S_A}$ values have been labeled Actual $\beta_{S_A}$ values in Table 1. Also shown in Table 1 are the $\beta'_{S_A}$ values obtained from Equation (2) using $\beta_{SAR} = 0.36$ and the $\beta_{AF}$ values listed in Table 1. When $\overline{S}_A$ is chosen as the interface parameter, $\beta'_{S_A}$ closely approximates $\beta_{S_A}$ over the entire frequency range of interest (i.e., the ignored cross-correlation is negligible). However, when PGA is chosen as the interface parameter, $\beta'_{S_A}$ severely overpredicts $\beta_{S_A}$ at frequencies below about 15 Hz (i.e., the ignored cross-correlation is significantly negative). Based on the several reasons discussed herein, but primarily based on this negligible cross-correlation in the 3 to 30 Hz range, we consider $\overline{S}_A$ to be a substantially preferable hazard/fragility interface parameter over PGA.

REFERENCE FOR ITEM 13

1. **Final Report of the Diablo Canyon Long-Term Seismic Program,** Pacific Gas and Electric Company, July 1988.

## Table 1

## Estimated Variabilities

| Frequency | SAR = $\overline{S}_A$ | | SAR = PGA | | Actual $\beta_{S_A}$ |
|---|---|---|---|---|---|
| | $\beta_{AF}$ | $\beta'_{S_A}$ | $\beta_{AF}$ | $\beta'_{S_A}$ | |
| 33 | 0.18 | 0.40 | 0.13 | 0.38 | 0.36 |
| 20 | 0.18 | 0.40 | 0.17 | 0.40 | 0.37 |
| 10 | 0.18 | 0.40 | 0.24 | 0.43 | 0.38 |
| 5 | 0.18 | 0.40 | 0.30 | 0.47 | 0.40 |
| 3.33 | 0.18 | 0.40 | 0.34 | 0.50 | 0.42 |

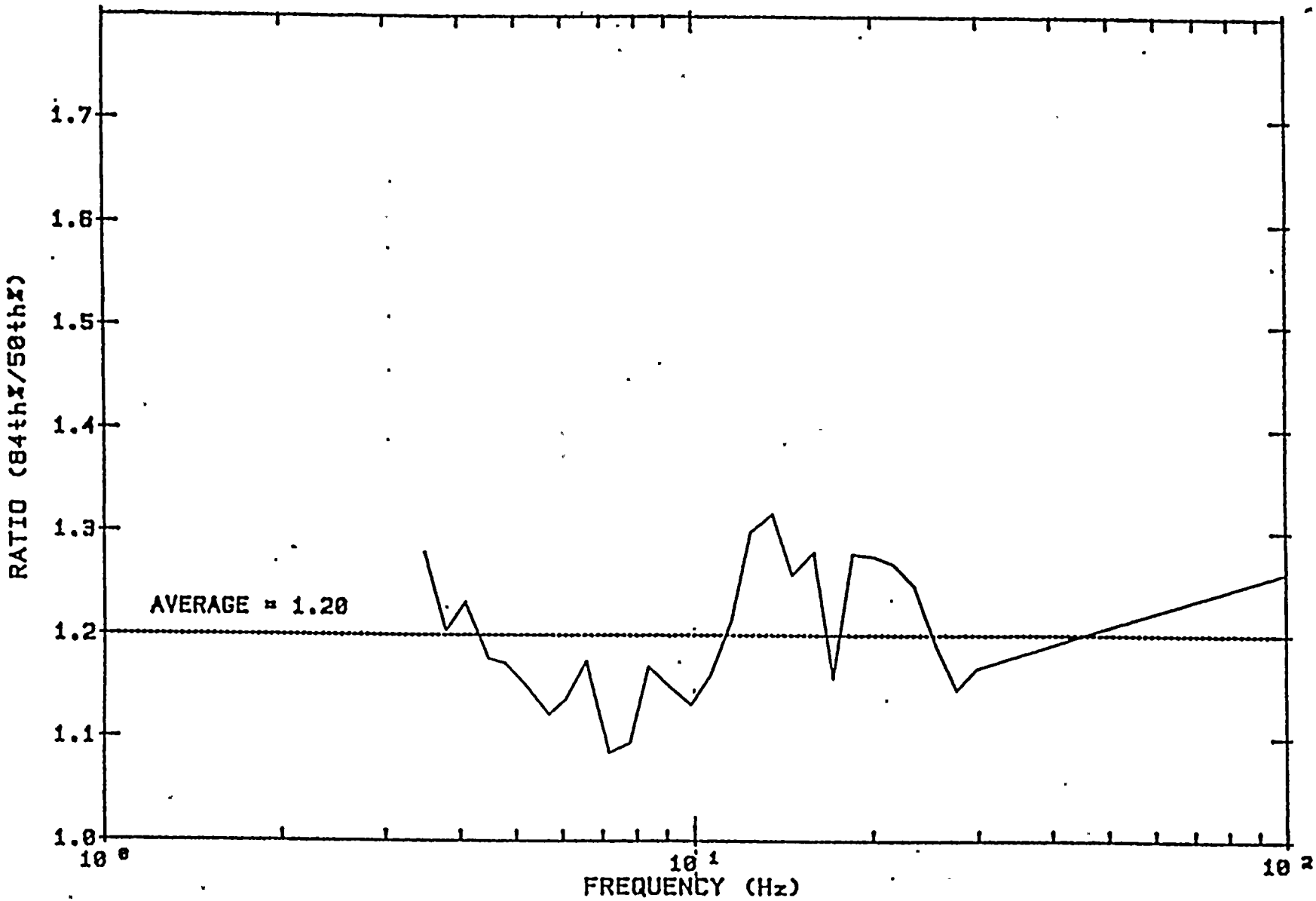


Figure 1. Peak-Valley Variability when anchored to $\overline{S}_{a\ 4.8\ Hz\ to\ 14.7\ Hz}$

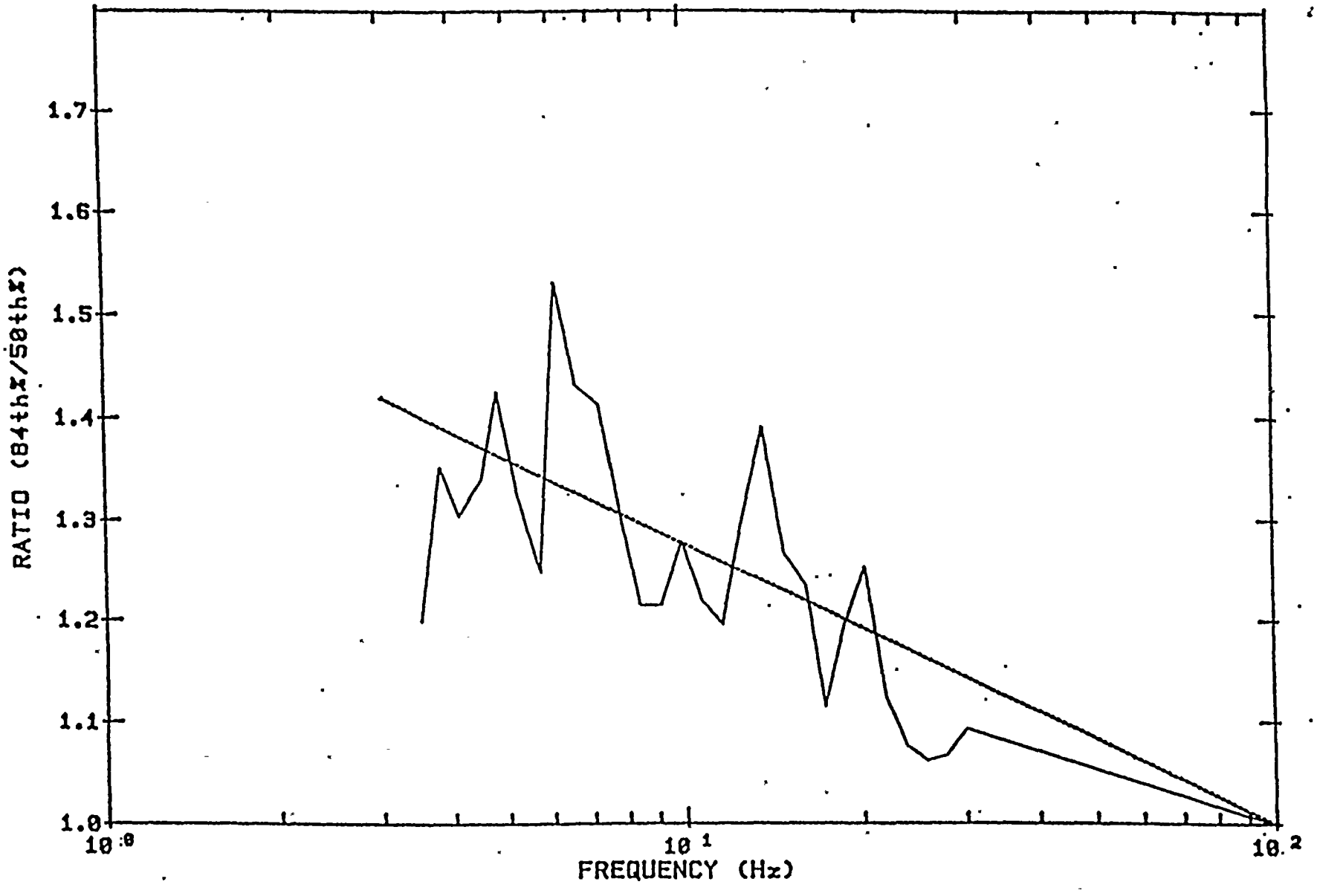


Figure. 2. Peak-Valley Variability when anchored to Peak Ground Acceleration

# APPENDIX A

# ESTIMATING FRAGILITIES FOR EQUIPMENT QUALIFIED BY TEST

# ESTIMATING FRAGILITIES FOR EQUIPMENT QUALIFIED BY TEST

R. P. Kennedy

July 1989

## INTRODUCTION

One of the more difficult and controversial tasks in a Seismic Probabilistic Risk Assessment (PRA) is the estimation of a seismic fragility for equipment for which one has only a seismic qualification test report showing that the equipment did not fail when subjected to a specific Test Response Spectrum (TRS) applied at the support points for the equipment. At these same support points, the seismic fragility test response spectrum ($TRS_F$) can be expressed by:

$$TRS_F = TRS \cdot F_{TET} \tag{1}$$

where $F_{TET}$ is a test exceedance factor which is both random and uncertain. The difficulty arises in estimating the median value, random and uncertainty logarithmic standard deviations, and High-Confidence-Low-Probability (HCLP) value for $F_{TET}$. Once the random variable, $F_{TET}$, is estimated, then the random variable, $TRS_F$, at the equipment supports can be converted to a seismic fragility expressed in terms of a ground motion parameter such as average spectral acceleration over a frequency range ($\overline{S}_A$) through the use of structural factors similar to those used for other equipment.

## FUNCTIONAL FAILURE MODE FRAGILITIES

Some functional failure modes of equipment are not accompanied by prior warning from structural distress being initiated at a lesser shaking level. In other words, those functional failure modes do not require visible structural distress. Examples of such failure modes are relay, contactor, or switch chatter, and electrically or mechanically induced breaker trip. For such failure modes, Lawrence Livermore National Laboratories (LLNL) has recommended that the following values be used for $F_{TET}$ (References 1 and 2):

LLNL

Median = 1.56

$\beta_R = 0.09$

$\beta_U = 0.18$

HCLP = 1.0

The variabilities $\beta_R$ and $\beta_U$ and the ratio of median to HCLP of 1.56 are completely consistent with my own observations and judgment, and I fully support the use of those estimates. However, I do not believe that the TRS from a single qualification test represents an HCLP value. Certainly, the fact that one item of equipment did not fail during one test does not give me 95% confidence of less than 5% probability of failure. The HCLP value should be estimated from:

$$\frac{HCLP}{TRS} = \frac{1}{F_K}$$

where $F_K$ is a knockdown factor which, at this time, must be judgmentally estimated. The LLNL judgment is that $F_K$ is 1.0. My judgment is that $F_K$ should be about 1.1. Based on my judgment, a realistic estimate for $F_{TET}$ would be:

Realistic

Median = 1.42

$\beta_R = 0.09$

$\beta_U = 0.18$

HCLP = 0.91

which represents a "knockdown" of the LLNL recommended values by a factor of 1.1.

Because of the relatively weak data base available to backup the estimates for $F_{TET}$, I have often recommended that the SPRA studies $F_{TET}$ be conservatively estimated as follows:

Conservative

Median = 1.2

$\beta_R = 0.08$

$\beta_U = 0.09$

HCLP = 0.91

In this estimate, the Median estimate has been scaled down to an "assuredly" low estimate which can be easily defended, while the HCLP is retained because it is already defensibly low. In this process, the variabilities must be reduced from their realistic values in order to obtain the proper relationship between the Median and the HCLP values.

## STRUCTURAL FAILURE MODE FRAGILITIES

Many functional failure modes of equipment require severe structural distress as an initiator. An example is dropping or disconnecting the breaker in a switchgear cabinet. These failures require an amount of relative displacement which is only credible if a structural support or structural connection totally fails. Another example is burnout of the core or disconnection of the dry transformer in a transformer cabinet. Again, these failures require sufficient relative movement, which is only credible after the failure of a structural connection or support if the transformer is anchored to the cabinet before the shaking. Such structural failures are preceded by structural anomalies or distress at lesser shaking levels. Thus, if no anomalies or distress such as cracking of welds, ripping out of sheet metal screws, or minor permanent distortion of sheet metal skins or structural framing are reported at the qualification TRS level, then an additional margin exists beyond that described in the functional failure modes in the previous section. In fact, many examples exist within both the seismic qualification of equipment testing programs and within the earthquake experience data base where each

of the above-mentioned anomalies or distresses have severely occurred without impairment of the equipment function. In my judgment, if none of these anomalies are reported at the TRS level, then a modified $F'_{TET}$ given below should be used in Equation (1):

$$F'_{TET} = F_{TET} \cdot F_{SF} \tag{3}$$

where $F_{SF}$ is a structural failure mode factor. A reasonable and probably somewhat conservative estimate for $F_{SF}$ would be:

$F_{SF}$

Median = 1.5

HCLP = 1.25

$\beta_U = 0.11$

**DIABLO CANYON LONG-TERM SEISMIC PROGRAM**

Table 1 summarizes the previous recommended estimates for $F_{TET}$. In addition, this table shows the values for $F_{TET}$ which have been used in the SPRA during the Diablo Canyon Long-Term Seismic Program (LTSP). In my opinion, the LTSP Median estimate is quite conservative, but the variability estimates $\beta_R$ and $\beta_U$ are low so that the HCLP estimates are either reasonable or slightly liberal.

However, $F_{TET}$ is only one parameter which goes into defining the fragility in terms of a ground motion hazard parameter ($\overline{S}_A$). There are many additional sources of variability in the various response parameters. It turns out that the Median estimate of $F_{TET}$ has a strong and directly proportional influence on both the Median and HCLPF $\overline{S}_A$, but the variabilities $\beta_R$ and $\beta_U$ for $F_{TET}$ have only a small influence on $\beta_R$ and $\beta_U$ for $\overline{S}_A$ because they are not the primary sources of variability. Thus, the HCLPF $\overline{S}_A$ is only slightly influenced by $\beta_R$ and $\beta_U$ for $F_{TET}$, and the Median $\overline{S}_A$ is not influenced at all. To illustrate this point, Table 2 presents the fragility estimate in terms of $\overline{S}_A$ for the Diablo Canyon 125-volt Switchgear. The LTSP values shown in Table 2 are the values reported in the Diablo Canyon LTSP fragility report. The Realistic and Conservative values are the fragility values I recomputed using the corresponding $F_{TET}$ values in Table 1 for structural failure modes in lieu of the LTSP. Use of more realistic

values for $F_{TET}$ would increase the LTSP median fragility estimate by 18% and the HCLPF estimate by 7%, despite the higher variabilities used. Even when my conservative values are used for $F_{TET}$, the LTSP HCLPF fragility estimate would only be reduced 3%.

In conclusion, the LTSP estimates for $F_{TET}$ results in a conservative estimate for the median $\overline{S}_A$ and a reasonable estimate of the HCLPF $\overline{S}_A$. In fact, either the Realistic, Conservative, or LTSP estimates for $F_{TET}$ can be used without introducing a significant effect on the HCLPF $\overline{S}_A$, the Seismic Margin, or the Seismic Risk.

## REFERENCES


1. Holman, G. S., and C. K. Chou, **Component Fragility Research Program--Phase I Component Prioritization**, NUREG/CR-4899, Lawrence Livermore National Laboratory, Prepared for U.S. Nuclear Regulatory Commission, June 1987.

2. Tsai, N. C., G. L. Mochizuki, and G. S. Holman, **Component Fragility Research Program--Phase II Development of Seismic Fragilities from High Level Qualification Data** (draft), Lawrence Livermore National Laboratory, Prepared for U.S. Nuclear Regulatory Commission, June 1989.

## Table 1

## Recommended Estimates for $F_{TET}$

### FUNCTIONAL

| | Median | $\beta_R$ | $\beta_U$ | HCLP |
|---|---|---|---|---|
| LLNL | 1.56 | .09 | .18 | 1.0 |
| Realistic | 1.42 | .09 | .18 | 0.91 |
| Conservative | 1.2 | .08 | .09 | 0.91 |
| LTSP | 1.2 | .05 | .10 | 0.94 |

### STRUCTURAL

| | Median | $\beta_R$ | $\beta_U$ | HCLP |
|---|---|---|---|---|
| Realistic | 2.13 | .09 | .21 | 1.30 |
| Conservative | 1.8 | .08 | .14 | 1.25 |
| LTSP | 1.8 | .05 | .11 | 1.38 |

## Table 2

### Fragility Estimates for 125-Volt Switchgear in Terms of $\overline{S}_A$

| | Median (g) | $\beta_R$ | $\beta_U$ | HCLP (g) |
|---|---|---|---|---|
| LTSP | 6.67 | .35 | .28 | 2.36 |
| Realistic | 7.89 | .36 | .33 | 2.53 |
| Conservative | 6.67 | .36 | .29 | 2.28 |

# APPENDIX B

# BASES FOR THE EVALUATION OF VARIABILITIES

## BASES FOR THE EVALUATION OF VARIABILITIES

The following discussion describes the bases for the evaluation of the variabilities in the equipment fragility analysis. This discussion focuses on the justification and judgment used to estimate the contributions of randomness and uncertainty to the overall variability. To present this material, the evaluation of the variabilities for two example components are reviewed. The fragility evaluation for the two components, the Reactor Coolant Pump and the Diesel Generator Control Panel, are both described in Reference 1. In this discussion, the evaluation of the variabilities is addressed in detail and covers both structural and functional failure modes. For the Reactor Coolant Pump, the fragility is based on a structural failure mode evaluated by analysis. For the Diesel Generator Control Panel, both the structural and functional fragilities are based on qualification test data.

### 1. REACTOR COOLANT PUMP

The critical failure mode for the RCP is associated with an excessive bending failure of the lower motor stand. A plastic hinge must form in the lower motor stand in order to develop the large horizontal displacements of the motor and the corresponding vertical displacements of the pump shaft which would lead to seal leakage.

### 1.1 Equipment Capacity Factors

Strength Factor

In Reference 1, the median Strength factor of safety was evaluated as

$$F_S = \frac{1.25(36.0) - 0.55}{32.03} = 1.39$$

in which 32.03 is the stress, in ksi, induced in the motor stand by the earthquake accelerations, 36.0 ksi is the minimum specified yield stress of the material, 1.25 is the ratio between the median and minimum material yield stress, and 0.55 ksi is the dead load stress.

The variabilities associated with the strength factor are all considered uncertainty, of which there are three main sources: (1) material yield stress, (2) uncertainty in the median earthquake stresses developed from the estimated median floor spectra at El 114 ft, and (3) the stress level required to form the plastic hinge mechanism.

In estimating the median yield stress, the ratio of the median to minimum yield stress was taken to be 1.25. Reference 2 gives this as an appropriate value for the median increase factor for carbon and stainless steels. It was judged that the code minimum represents a 95% confidence (i.e., a -1.65 $\beta$) lower bound. Therefore,

$$\beta_{U_{1.25}} = \frac{1}{1.65}\ln(1.25/1.00) = 0.14$$

To establish the median seismic stresses in the motor stand, the median floor spectra at El 114 ft had to be estimated, since the median spectra were only generated at El 140 and 85 ft. The median spectra at El 114 ft were interpolated from the 140 and 85 ft spectra using the relative Hosgri spectral accelerations. The interpolation was based on the expectation that the ratio of the median spectra to the Hosgri spectra at their respective peak frequencies should be similar at all elevations or at least exhibit a trend that could be interpolated. This same expectation was held for the frequencies when expressed as a ratio of the peak frequencies. To estimate the uncertainty associated with the interpolation, it was judged that an increase of 20% (i.e. scaling by 1.2) in the interpolated spectral accelerations represented a 95% confidence upper bound. This was felt to be a reasonable estimate since the interpolation included the relative spectral accelerations as well as the relative amplification with respect to the peak frequencies. Therefore, the uncertainty associated with the estimated spectral accelerations used to calculate the median seismic stresses was evaluated as

$$\beta_{U_{S_a}} = \frac{1}{1.65}\ln(1.20/1.00) = 0.11$$

The development of the failure mode is dependent on attaining large horizontal displacements resulting from the formation of a plastic hinge in the cut-out portion of the motor stand. In order to develop the displacements, a large amount of plastic deformation is required. The shape factor for the cut-out section (the ratio of the plastic to elastic section modulus) was calculated to be 1.46, which indicates that there is substantial margin between the development of first yield in the section and the formation of a plastic hinge. However, due to slight irregularities in the geometry of the section, the plastic hinge may form at a bending moment slightly less than the theoretical plastic moment. Because there is substantial inelastic capacity between first yield and the plastic moment and because the section is essentially circular, it was judged that a 95% confidence lower bound for the formation of the plastic hinge could be represented as the point at which the section was 90% fully plastic. That is, there is an estimated 95% confidence that a plastic hinge would not form until the section is at least 90% fully plastic. Therefore,

$$\beta_{UP} = \frac{1}{-1.65}\ln(0.90/1.00) = 0.06$$

The variabilities in the strength factor are then given by

$$\beta_{SR} = 0.0$$

$$\beta_{SU} = (0.11^2+0.14^2+0.06^2)^{1/2} = 0.19$$

Inelastic Energy Absorption Factor

The Inelastic Energy Absorption factor was evaluated from the elastic and plastic displacements of the center of gravity of the motor assuming a median strain in the cut-out section of 0.04 at failure. This produced a median ductility of 3.51. As described in Reference 1, the median value of $\hat{F}_{\mu}$ was calculated to be 2.77 using the median ductility of 3.51 and the relationships in Reference 4. Using the results of analyses on the influence of the ground motion characteristics on the inelastic spectral deamplification contained in Reference 3, the randomness variability is estimated from

$$\beta_R = 0.11(\hat{F}_\mu - 0.50)$$

$$= 0.11(2.77 - 0.50) = 0.25$$

There is also uncertainty in the Inelastic Energy Absorption factor. To evaluate this uncertainty, an estimate of the variability in the ductility factor is required. This was accomplished using the judgment that a strain at failure of 0.025 constitutes a 95% confidence lower bound. An estimate of the uncertainties in the elastic displacements was also required to evaluate $\beta_\mu$. The overall logarithmic standard deviation of the ductility factor was estimated to be 0.31. Therefore, the -1$\beta$ value of the Ductility factor was evaluated as

$$\mu_{-1\beta} = \hat{\mu} e^{-\beta}$$

$$= 3.51 e^{-0.31} = 2.57$$

Using the above value of $\mu_{-1\beta}$, the corresponding -1$\beta$ value for $F_\mu$ was calculated to be 2.34 using the expressions for the inelastic deamplification factors of Riddell and Newmark (Reference 4). Therefore, the uncertainty in the Inelastic Energy Absorption factor was evaluated from

$$\beta_U = \ln(2.77/2.34) = 0.17$$

Overall Equipment Capacity Factor

Combining the median values and the variabilities from the Strength factor and the Inelastic Energy Absorption factor, the median value and the variabilities for the Equipment Capacity factor are

$$\hat{F}_{EC} = (1.39)(2.77) = 3.85$$

$$\beta_{EC_R} = 0.25$$

$$\beta_{EC_U} = (0.19^2 + 0.17^2)^{1/2} = 0.25$$

## 1.2 Equipment Response Factors

Qualification Method Factor

Since the Strength factor was evaluated based on stresses computed by an equivalent static analysis using the 5% damped reference spectra, the stresses are median centered. Therefore, the median value of the Qualification Method factor is 1.00 and the associated variabilities are zero.

Damping Factor

The Strength factor was based on the reference spectra with 5% damping, which is judged to be median centered at or near failure. Therefore, the median Damping factor is 1.00. All of the variability in the Damping factor is treated as uncertainty. In particular, there is uncertainty in the damping level at failure. Reference 5 suggests that the median damping for equipment at the SSE level is about 5% and that the -1β damping value is 3.5%. From the Auxiliary Building variability study and the generation of median floor spectra for the Auxiliary Building, floor spectra were developed for damping values of 3, 5, 7, and 15%. Spectra with 3.5% damping were interpolated from these spectra. From a comparison of the uncertainty variability in the 3.5% damped spectra, it was found that the variation between the 3% and 5% damped spectra represented a -1.33 β variation. This variation was found to be consistent and accurate for all elevations. Therefore, it was judged that, with 5% as a median value, a damping value of 3% represented a -1.33 β lower bound.

However, damping and inelastic energy absorption are interrelated and part of the reduced response attributed to inelastic behavior is actually related to higher damping levels. As a result, part of the variability already considered in the Ductility factor is actually associated with the uncertainty in the damping. Therefore, to avoid counting this uncertainty twice, the damping uncertainty is evaluated as

$$\beta_{DU} = \frac{1}{1.33}\ln\left[\left(\frac{S_{a3\%}}{S_{a5\%}}\right)\left(\frac{F_{\mu 5\%}}{F_{\mu 3\%}}\right)\right]$$

$$= \frac{1}{1.33}\ln\left[(1.22)\left(\frac{2.77}{2.99}\right)\right] = 0.09$$

$$\beta_{DR} = 0.0$$

Modeling Factor

The Modeling factor accounts for the uncertainty in calculating the proper mode shape and frequency of the equipment. All of the variability associated with the Modeling factor is treated as uncertainty. The logarithmic standard deviation associated with the equipment mode shape is taken to range from 0.05 to 0.15. This range is based on values suggested in Reference 6, where the higher value of 0.15 corresponds to complex multi-degree-of-freedom systems. Since the RCP is expected to respond primarily in its fundamental mode and it is essentially a single degree of freedom system, a mode shape uncertainty of 0.10 was judged appropriate. Therefore,

$$F_{MS} = 1.00$$

$$\beta_{MSR} = 0.0$$

$$\beta_{MSU} = 0.10$$

The variability due to frequency has contributions from both the uncertainty in equipment frequency and the uncertainty in structure frequency. The equipment frequency variability typically ranges from 0.09 to 0.20 based on the results of Reference 5. The upper bound value corresponds to a complex component whose frequency was established by approximate methods. The frequency of the RCP was determined from a finite element beam model and thus, the logarithmic standard deviation of the RCP frequency was taken to be 0.15. The uncertainty associated with frequency of the Containment Building Internal Structure, in addition to that included in the Structural Response factor, was taken as 0.15. Therefore, the overall frequency uncertainty was estimated as

$$\beta_{fU} = (0.15^2 + 0.15^2)^{1/2} = 0.21$$

However, this frequency uncertainty alone does not measure the effect on the equipment response. The frequency variability is used to evaluate the ± 1 β frequency range about the median, within which the variation of the spectral accelerations is examined. Generally, the variation of the spectral acceleration within the ± 1 β frequency range is also taken to be a ± 1 β variation.

With the median fundamental frequency of the reactor coolant pump having a value of 6.9 Hz, the ± 1 β frequency values are evaluated as

$$f_{-1\beta} = 6.9e^{-0.21} = 5.6Hz$$

$$f_{1\beta} = 6.9e^{0.21} = 8.5Hz$$

The median frequency falls on the low frequency side of the horizontal floor spectra, which peak at a frequency of about 8 Hz for both the NS and EW directions. By considering a ± 1 β frequency shift about the median, the global maximum horizontal spectral accelerations are included in the frequency range. From 5.6 to 8.5 Hz, the median horizontal spectral floor acceleration vector is 3.36g and the maximum vector is 4.28g. These vector magnitudes were calculated from the orthogonal horizontal components based on 100% of the NS spectral acceleration and 40% EW spectral acceleration. In the evaluation of the Strength factor, the directional responses were combined using the median centered 100/40/40 method. Also, in the evaluation of the Strength factor, a spectral acceleration vector of 3.25g was used. There is a slight unconservatism in the Strength factor. The median Modeling factor associated with frequency is

$$F_M = (3.25/3.36) = 0.97$$

Because the ± 1 β frequency range included the global maxima of the horizontal floor spectra, the modeling uncertainty associated with frequency was estimated by considering the maximum horizontal spectral acceleration vector in the ± 1 β frequency range to be a 2.33β upper bound (99% confidence bound). The modeling uncertainty associated with frequency then becomes

$$\beta_{fU} = \frac{1}{2.33}\ln\left(\frac{4.28}{3.36}\right) = 0.10$$

Noting that the variabilities associated with the Modeling factor are all treated as uncertainty and combining the contributions from both the frequency and mode shape, the median Modeling factor and its variabilities are

$$\hat{F}_M = 0.97$$

$$\beta_{M_R} = 0.0$$

$$\beta_{M_U} = (0.10^2 + 0.10^2)^{1/2} = 0.14$$

Mode Combination Factor

The response of the RCP is essentially all due to the fundamental mode. In addition, the directional responses are uncoupled. Therefore, it was judged that the analytical model could adequately represent the actual response from all of the modes excited by the seismic input. A nominal randomness of 0.05 was assigned for the Mode Combination factor. Thus,

$$\hat{F}_{MC} = 1.00$$

$$\beta_{MC_R} = 0.05$$

$$\beta_{MC_U} = 0.0$$

Earthquake Component Combination Factor

The Strength factor was based upon stresses computed using the median centered 100%/40%/40% method to combine the earthquake components. Therefore, the median value of $F_{ECC}$ is 1.00. In order to evaluate the randomness variability, it was judged that a combination of 100%/60%/40% represents a + 1 β response level. This variability accounts for the random phasing of the earthquake components, noting that both of the horizontal components contribute to failure. For the 100%/60%/40% combination, the stress was 34.39 ksi. Therefore,

$$\hat{F}_{ECC} = 1.00$$

$$\beta_{ECC_R} = \ln(34.39/32.03) = 0.07$$

$$\beta_{ECC_U} = 0.0$$

Overall Equipment Response Factor

The median value and the associated variabilities of the overall Equipment Response factor are obtained by combining the constituent parts, which gives

$$\hat{F}_{ER} = 0.97$$

$$\beta_{ER_R} = \left(\beta_{MC_R}^2 + \beta_{ECC_R}^2\right)^{1/2}$$

$$= (0.05^2 + 0.07^2)^{1/2} = 0.09$$

$$\beta_{ER_U} = \left(\beta_{D_U}^2 + \beta_{M_U}^2\right)^{1/2}$$

$$= (0.09^2 + 0.14^2)^{1/2} = 0.17$$

## 1.3 Structural Response Factors

Structural Spectral Shape Factor

As noted in Reference 1, the variabilities of the Structural Spectral Shape factor were based on the results of the Auxiliary Building Variability study. Composite variabilities at the various elevations for different frequency bands were estimated from the 84th and 50th percentile floor spectra. These variabilities are composite values since the Auxiliary Building Variability study included the effects of both the randomness of the earthquake ground motion and the uncertainty in the structural model. Since the RCP is located at elevation 114 ft, the response variabilities must be interpolated between values for the basemat at El 85 ft and the operating floor at El 140 ft. The variability of the Structural Spectral Shape factor was evaluated

using the $\beta_C$ values for the low frequency range (3.5 -5 Hz) because it was judged that the nonlinear response of the RCP at failure would drive the frequency down into this range. In the low frequency range, $\beta_C$ has a value of 0.24 at the basemat level and a value of 0.27 at elevation 140. Interpolating between these two values to obtain the composite variability at El 114 ft,

$$\beta_{C_{114}} = \left(\frac{114-85}{140-85}\right)(0.03)+0.24 = 0.26$$

At elevations above the basemat, most of the increase in the composite variability over the basemat value can be attributed to uncertainty in the structural properties. Therefore, the randomness and uncertainty variabilities are separated out of the composite variability as

$$\beta_{SS_R} = 0.24+0.01 = 0.25$$

$$\beta_{SS_U} = (0.26^2-0.25^2)^{1/2} = 0.07$$

and

$$\hat{F}_{SS} = 1.00$$

Structural Mode Shape Factor

Based on the judgment that the analytical model of the Containment Building Internal Structure was developed using the best effort of the analyst, the median value of the Structural Mode Shape factor is unity. The uncertainty in the structure mode shape at or above the C.G. is taken to be 0.15. This is based on the value suggested in Reference 5 for complex, multi-degree-of-freedom systems. Between the basemat and the C.G., the uncertainty is evaluated by interpolation. Therefore,

$$\hat{F}_{MS} = 1.00$$

$$\beta_{MS_R} = 0.0$$

$$\beta_{MS_U} = \left(\frac{114-85}{140-85}\right)(0.15) = 0.08$$

Ground Motion Incoherency

The Ground Motion Incoherency factor accounts for the conservatism associated with the assumption of a spatially coherent ground motion acting on the structure foundation. This effect is most apparent for structures with long basemat plan dimensions. As part of the LTSP Soil-Structure Interaction study, comparisons were made between the floor spectral accelerations using coherent and incoherent ground motions. The ratio of the spectral acceleration at El 114 ft. for incoherent earthquake motion to that for coherent motion had a value of 0.95. Thus, the median factor of safety has a value of 1/0.95 or 1.05. As defined in Reference 1, the composite variability was estimated as

$$\beta_{GMI_C} = \frac{1}{1.65} \ln\left(\frac{1.05}{1.00}\right) = 0.03$$

The randomness and uncertainty are separated out from the composite variability as

$$\beta_{GMI_R} = 0.6\beta_{GMI_C} = 0.02$$

$$\beta_{GMI_U} = 0.8\beta_{GMI_C} = 0.02$$

Inelastic Structural Response Factor

As a structure begins to yield and respond inelastically, the spectral accelerations tend to reduce relative to the scaled linear spectra at frequencies near the peak of the floor spectra. However, it has been observed that, at higher frequencies, the inelastic spectral accelerations can show an increase over the scaled linear spectra. Whether the inelastic spectral accelerations are higher or lower than the scaled linear spectra depends on the dynamic characteristics of the structure and the frequency content of the earthquake ground motion. To include this effect for high frequency components, a composite variability, $\beta_C$, of 0.20 was taken to represent the variability due to the inelastic structure response at or above the C.G. of the structure. This value for $\beta_C$ was judged appropriate based on the results of a study addressing the effects of ground motion characteristics on structural response (Reference 7). The randomness and uncertainty variabilities were separated from the composite value as $\beta_{IR_R} = 0.17$ and $\beta_{IR_U} = 0.10$.

While the variabilities described above are applicable to high frequency components, they are not directly applicable to the Reactor Coolant Pump. The median fundamental frequency of the RCP has a value of 6.9 Hz, which lies on the soft (low frequency) side of the peak of the floor spectra. As a result, it is less likely that the inelastic spectral accelerations will exceed the scaled elastic spectra in this lower frequency range. Therefore, a lower value of $\beta_C$ equal to 0.10 was used to account for the variability in the inelastic spectra at or above the vertical C.G. of the structure. The randomness and uncertainty variabilities were separated from the composite variability in the same proportions as for the high frequency case, with $\beta_{IR_R} = 0.085$ and $\beta_{IR_U} = 0.05$.

Since the RCP is located at El 114 ft which is between the basemat and the C.G., the variabilities of the Inelastic Structural Response factor are interpolated from the above values as

$$\beta_{IR_R} = \left(\frac{114-85}{140-85}\right)(0.085) = 0.05$$

$$\beta_{IR_U} = \left(\frac{114-85}{140-85}\right)(0.05) = 0.03$$

Overall Structural Response Factor

The combined Structural Response factor and its variabilities are

$$\hat{F}_{SR} = 1.05$$

$$\beta_{SR_R} = (0.25^2 + 0.02^2 + 0.05^2)^{1/2} = 0.26$$

$$\beta_{SR} = (0.07^2 + 0.08^2 + 0.02^2 + 0.03^2)^{1/2} = 0.11$$

Ground Spectral Acceleration Capacity

As in Reference 1, the median ground spectral acceleration capacity of the Reactor Coolant Pump is evaluated as

$$\tilde{S}_a = (3.85)(0.97)(1.05)(2.00g)(1.125) = 8.82g$$

The associated logarithmic standard deviations for randomness and uncertainty are computed by taking the SRSS combination of the variabilities of the Equipment Capacity factor, the Equipment Response factor, and the Structural Response factor.

$$\beta_R = (0.25^2 + 0.09^2 + 0.26^2)^{1/2} = 0.37$$

$$\beta_U = (0.25^2 + 0.17^2 + 0.11^2)^{1/2} = 0.32$$

## 2. DIESEL GENERATOR CONTROL PANEL

The fragility of the Diesel Generator Control Panel was developed from qualification test data. The failure modes of the panel are associated with both a functional failure from relay chatter and structural failure of the cabinet leading to a loss of function. In the fragility analysis, it was found that the chatter failure had substantially higher capacity than the structural failure mode. Therefore, the loss of function resulting from a generic structural failure was the governing failure mode and this fragility was used in the risk analysis.

In this example, the evaluation of the variabilities for both the functional anc structural failure modes are described for each of the respective factors.

## 2.1 Equipment Capacity Factor

Strength Factor

For electrical equipment qualified by shake table testing, the component is subjected to test table motions such that the response spectrum of the input motion envelopes the required floor response spectrum. The tests are not carried to a failure level and, therefore, are not fragility tests in themselves. When no structural distress or contactor chatter is observed in the test, the actual median acceleration capacity is somewhat above the qualification acceleration level.

Unlike most electrical cabinets qualified by tests, the Diesel Generator Control Panel was tested in a slightly different configuration than the plant installation. For the dynamic test, the vertical cabinet with front-to-back bracing was tested alone. The resulting side-to-side frequency was 5 Hz and was governed by the flexibility of the shock isolation mounts. The in-situ installation includes the vertical cabinet plus an additional light weight horizontal cabinet which is also shock mounted and is bolted to the vertical cabinet. The horizontal side-to-side frequency of the in-situ configuration is approximately 7.9 Hz.

No structural distress was noted in the qualification of the control panel. Thus, appropriate increase factors are required to estimate the margin between the median acceleration capacity for structural failure and the qualification acceleration level. Two factors are involved. First, the yield level of the critical element is estimated to be a factor of 1.2 above the qualification level. Second, the median failure level is estimated to be a factor of 1.5 higher than the yield level. Since the strength factor of safety is measured relative to the reference earthquake response spectrum, the median Strength factor is evaluated from

$$F_S = (1.2)(1.5)\frac{S_{a\,TRS}}{S_{a\,RRS}}$$

in which $S_{a\,TRS}$ is the test spectral acceleration evaluated at the tested cabinet frequency (i.e., 5 Hz) and $S_{a\,RRS}$ is the reference spectral acceleration evaluated at the in-situ cabinet frequency (i.e., 7.9 Hz). The test response spectra were analyzed for 3% damping. Therefore, the reference spectral accelerations, which were given for 5% damping, were adjusted to 3% damping in order that the acceleration overtest ratio could be evaluated at like damping values.

The Diesel Generator Control Panel is braced at the top by a Unistrut framework such that the front-to-back response is restrained. As a result, the panel responds in primarily a biaxial side-to-side and vertical mode. Therefore, the east-west (side-to-side) and vertical earthquake components are judged to govern the structural failure. Comparing the TRS about the tested cabinet frequency of 5.0 Hz to the east-west (side-to-side) reference floor spectrum about the in-situ cabinet frequency of 7.9 Hz resulted in a median overtest factor of 1.12. However, in the vertical direction, because the reference vertical ground spectrum is much higher than the Hosgri vertical spectrum at the cabinet vertical frequency of 22 Hz, the median overtest factor was found to be only 0.53. An evaluation of several critical failure modes of the panel revealed that if the vertical overtest factor had been equal to the side-to-side overtest factor, there would not be a significant impact on the total stress. Therefore, the Strength factor was based on the side-to-side overtest factor, yielding

$$F_S = (1.2)(1.5)(1.12) = 2.02$$

The variabilities in the Strength factor are derived from the increase factors. The variability in setting the median yield level at 1.2 times the test level is estimated by assuming that the test level represents a 95% confidence lower bound (-1.65β) for the yield level. The composite variability in the yield level is then calculated from

$$\beta_{1.2C} = \frac{1}{-1.65}\ln(1.0/1.2) = 0.11$$

The variability in the yield level is influenced somewhat by the characteristics of the seismic input, but is judged to be primarily uncertainty. Therefore, the logarithmic standard deviations associated with randomness and uncertainty are then separated from $\beta_{1.2C}$ as $\beta_R = 0.05$ and $\beta_U = 0.10$.

The variability in specifying the median failure capacity as 1.5 times the yield level is considered to be all uncertainty. The logarithmic standard deviation is estimated by taking a factor of 1.4 to represent a 95% confidence lower bound. The uncertainty is then evaluated as

$$\beta_U = \frac{1}{-1.65}\ln(1.4/1.5) = 0.04$$

By taking the factor of 1.4 to be a 95% confidence lower bound, a rather narrow distribution is defined. However, this is felt to be reasonable because the median factor of 1.5 is judged to be conservative.

The overall variabilities in the Strength factor for a structural failure are given by

$$\beta_{SR} = 0.05$$

$$\beta_{SU} = (0.10^2 + 0.04^2)^{1/2} = 0.11$$

For the functional failure mode, a review of the electrical components in the control panel conducted by PG&E indicated that only five relays have negative consequences should chatter occur. In addition, all five relays can be reset from the control room. Of these five, the most critical in terms of acceleration capacity was a Westinghouse ARD relay, which has a critical direction that coincides with the front-to-back direction of the cabinet. The acceleration capacity is derived from the Generic Equipment Ruggedness Spectrum (GERS) taken from Reference 8. The median acceleration capacity was estimated as 15% higher than the smooth GERS acceleration for the relay. As noted in Reference 1, the Strength factor of safety for relay chatter is taken as

$$F_S = \frac{1.15 \times GERS}{A_q \times S_a}$$

where $A_q$ is the amplification factor for the cabinet in the critical front-to-back direction and $S_a$ is the floor spectral acceleration evaluated at the fundamental front-to-back frequency of the cabinet.

From Reference 8, the GERS acceleration is 10g and is based on a 5% damped spectrum. At the front-to-back frequency of 19 Hz, the 5% damped north-south reference floor spectral acceleration is 1.28g. In the fragility analysis, a cabinet amplification factor of 3.0 was used since the relay is located relatively low in the cabinet on the interior relay panels and since the cabinet is braced in the front-to-back direction. Therefore, the median Strength factor becomes

$$F_s = \frac{1.15 \times 10.0}{3.0 \times 1.28} = 2.99$$

There is uncertainty in estimating the median capacity as 1.15xGERS. However, the GERS accelerations were developed to represent the maximum input motions for which existing test data verified the capability of the component to properly function during and after an earthquake. Therefore, the GERS itself does not constitute a failure level because the actual median failure acceleration is expected to be somewhat higher. As a result, the 1.15 factor is judged to be a conservative increase factor to represent median chatter failure. The uncertainty in the median capacity is estimated by considering the GERS to be a 95% confidence (-1.65 $\beta$) lower bound. This was felt to be reasonable in light of the basic definition of the GERS. The logarithmic standard deviation of the median capacity is evaluated as

$$\beta_U = \frac{1}{-1.65} \ln(1.0/1.15) = 0.08$$

An argument can be made for additional variability in the strength factor associated with the amplification factor, $A_q$. However, in the case of the Diesel Generator Control Panel, a very conservative amplification factor of 3.0 was used to evaluate the strength factor for the Westinghouse ARD relay. Noting that the top of the control panel is braced to an adjacent wall by a Unistrut framework such that the front-to-back response of the cabinet is restrained, it was judged that, the conservative amplification factor was nearly an upper bound and no variability needed to be accounted for.

Thus, the logarithmic standard deviations of the Strength factor for a functional failure are given by

$$\beta_{S_R} = 0.0$$

$$\beta_{S_U} = 0.08$$

Inelastic Energy Absorption Factor

For both the structural and functional failure modes, no additional credit was taken for ductility to increase the acceleration capacity. In the case of the structural failure mode, the generic failure condition could correspond to an non-ductile anchorage failure. For the functional failure, no credit can be taken for ductility in the case of contactor chatter, since this certainly does not represent ductile behavior. Therefore, the median factor is unity and the randomness and uncertainty variabilities are both zero.

Overall Equipment Capacity Factor

Since there is no contribution from the Inelastic Energy Absorption factor, the overall Equipment Capacity factor and its variabilities are equivalent to those for the Strength factor.

Structural

$\hat{F}_{EC} = 2.02$

$\beta_{EC_R} = 0.05$

$\beta_{EC_U} = 0.11$

Functional

$\hat{F}_{EC} = 2.99$

$\beta_{EC_R} = 0.0$

$\beta_{EC_U} = 0.08$

## 2.2 Equipment Response Factors

Qualification Method Factor

For the structural failure mode, the panel was qualified by random, multi-frequency shake table testing, which is taken to be median centered. For the functional failure mode,

because the strength factor was referenced to the median floor spectrum, the qualification method is previously accounted for. Therefore, for both the structural and functional failure modes the median factor is unity and the variabilities are zero.

Damping Factor

For both the structural and functional failure modes, the qualification was based on test levels in which the test damping values are median centered by definition. Moreover, in evaluating the strength factor, the test spectral accelerations are compared to the reference floor spectra at like values of damping. As a result, the median Damping factor is unity and the randomness and uncertainty variabilities are zero.

Boundary Conditions Factor

For components qualified by test, the variabilities associated with the Boundary Conditions factor reflect the variations in the response that are attributed to differences in the mounting conditions between the test fixture and the in-situ plant installation. In the qualification tests, the shake table mounting matched the floor anchored, shock isolator mounting used in the plant.

For the structural failure mode, the controlling side-to-side frequency is governed by the flexibility of the shock isolators. As a result, the variability in the fundamental frequency is expected to be low and a logarithmic standard deviation, $\beta_{f_e}$, of 0.10 was taken for the equipment frequency. Also, since the control panel is located on the basemat level of the Turbine building, there is no additional uncertainty contribution to the frequency due to the building response. The structural overtest factor was evaluated over a frequency range of $\pm 1.65\beta_f$ about the median side-to-side frequency of 7.9 Hz. This corresponded to frequencies between 6.7 and 9.3 Hz, since

$$f_{-1.65\beta} = 7.9e^{-1.65(0.10)} = 6.7Hz$$

$$f_{1.65\beta} = 7.9e^{1.65(0.10)} = 9.3Hz$$

Over this frequency range, the median overtest factor was found to be 1.12, while the minimum overtest factor was 1.01. Since the frequency range corresponded to a $\pm$ 1.65 $\beta$ range, the difference between the minimum and median overtest factor corresponds to a 1.65$\beta$ variation. The variability in the boundary conditions factor is considered to be uncertainty only and, thus, the logarithmic standard deviations for randomness and uncertainty for the structural failure mode are

$$\beta_{M_R} = 0.0$$

$$\beta_{M_U} = \frac{1}{-1.65}\ln(1.01/1.12) = 0.06$$

For the functional failure mode, the front-to-back direction is critical. However, due to the bracing of the cabinet in the front-to-back direction, the response uncertainty is judged to be minimal. Therefore, for the functional failure mode, the variabilities of the Boundary Conditions factor are

$$\beta_{M_R} = 0.0$$

$$\beta_{M_U} = 0.05$$

Spectral Test Methods Factor

The Spectral Test Methods factor characterizes the ability of the test method to sufficiently excite all important modes of the equipment. In the case of the structural failure mode, the biaxial test utilized random, multi-frequency motion. For the functional failure mode evaluation, the GERS was developed from existing test data for the relay which included triaxial, multi-frequency tests as well as uniaxial, narrow band tests. Therefore, the test methods were judged to be capable of exciting the important equipment modes. The median Spectral Test factor is unity and the associated variabilities are zero.

Earthquake Component Combination Factor

The Earthquake Component Combination factor quantifies the unconservatism in the use of the biaxial test to represent the actual earthquake response. In general, the equipment response has contributions from each of the three orthogonal earthquake components and, thus, a biaxial test is unconservative. However, because the control panel is braced in the front-to-back direction, the side-to-side direction governs the structural failure mode. The side-to-side and vertical biaxial test is then judged to be median centered for structural failure and the median factor of safety is unity.

An evaluation of three critical structural failure modes of the control panel (a 5/8" hold down bolt, a 1/2" vibration isolation anchor, and the worst case relay mounting screws) indicated that the vertical direction contribution was less than 25% of the side-to-side direction contribution to the critical response. The relative peak response contributions for the horizontal and vertical directions to the overall response was then taken to be 1.0 and 0.25, respectively. This relationship was used to estimate the randomness variability due to the phasing of the earthquake components. Since only the side-to-side and vertical directions contribute to the critical response, the absolute sum of the peak responses of the two components represents a maximum, worst case upper bound, while an SRSS combination of the components is median centered. Since the absolute sum is the maximum upper bound, it is judged to represent a 3 $\beta$ upper bound relative to the median. All of the variability is associated with the randomness of the earthquake input. Therefore, the variabilities in $F_{ECC}$ for the structural failure mode are

$$\beta_{ECC_R} = \frac{1}{3} \ln \frac{1.00 + 0.25}{(1.00^2 + 0.25^2)^{1/2}} = 0.06$$

$$\beta_{ECC_U} = 0.0$$

For the functional failure mode, the GERS was developed from triaxial multi-frequency tests both with and without an additional superimposed uniaxial narrow band input. Since the critical relay is sensitive to only the front-to-back direction, the median factor of safety for earthquake component combination is unity. Also, because only one direction contributes to failure, the variability due to random phasing is judged to be minimal. Therefore, the logarithmic standard deviations for randomness and uncertainty obtained for the structural failure mode were adopted for the functional failure mode.

Overall Equipment Response Factor

Combining the different contributing factors, the median Equipment Response factor and its variabilities are

Structural

$$\hat{F}_{EC} = 1.00$$
$$\beta_{EC_R} = 0.06$$
$$\beta_{EC_U} = 0.06$$

Functional

$$\hat{F}_{EC} = 1.00$$
$$\beta_{EC_R} = 0.06$$
$$\beta_{EC_U} = 0.05$$

## 2.3 Structural Response Factors

Since the Diesel Generator Control Panel is located at the basemat elevation of the Turbine Building, only the spectral shape and ground motion incoherency factors are applicable. The structure mode shape and inelastic structural response factors have no contribution for equipment located at the basemat level.

Structural Spectral Shape Factor

For both the structural and functional failure modes, the median Structural Spectral Shape factor has a median value of unity, since the Strength factor was based upon the reference spectra. As noted previously, the variabilities of the Structural Spectral Shape factor are based on the results of the Auxiliary Building variability study. In the vertical direction, the variabilities were based on the variabilities in the vertical ground motion as determined in the LTSP ground motion studies. These composite variabilities were weighted by the respective directional response contributions to obtain the overall composite variability in the Structural Spectral Shape factor.

For the structural failure mode, the side-to-side (east-west) and vertical directions governed the critical response. From Reference 1, the variability at the basemat level in the east-west direction is 0.28 at the cabinet side-to-side frequency of 7.9 Hz. For the vertical direction, the variability at the cabinet vertical frequency of 22 Hz is 0.35. Since the control panel is located on the basemat, the influence of the variability in the structure properties is not included. The overall variability in the Structural Spectral Shape factor is then judged to be all randomness. Using the relative response contributions of 1.00 and 0.25 for the east-west and vertical directions as in the equipment earthquake component combination factor, the randomness logarithmic standard deviation for the structural failure mode becomes

$$\beta_{SS_R} = \left[\frac{(1.00\times 0.28)^2+(0.25\times 0.35)^2}{1.00^2+0.25^2}\right]^{1/2} = 0.29$$

and

$$\beta_{SS_U} = 0.0$$

For the functional failure mode, only the front-to-back (north-south) direction contributes to the critical response. At the front-to-back cabinet frequency of 19 Hz, the composite variability at the basemat is 0.24 in the north-south direction as noted in Reference 1. Again, since the control panel is located on the basemat, this variability is all randomness. Therefore, the variabilities for the functional failure mode are

$$\beta_{SS_R} = 0.24$$

$$\beta_{SS_U} = 0.0$$

Ground Motion Incoherency Factor

For the structural failure mode, the east-west direction governs the critical response. However, due to the comparatively short length of the Turbine Building in the east-west direction, the effect of statistical incoherence of the ground motion is negligible in that direction. In the vertical direction, statistical incoherence is not applicable. Therefore, $\hat{F}_{CMI}$ is unity and the composite variability has a nominal value of 0.05. As described in Reference 1, the randomness and uncertainty $\beta$ values are separated from the composite variability as

$$\beta_{GMI_R} = 0.6\beta_C = 0.6(0.05) = 0.03$$

$$\beta_{GMI_U} = 0.8\beta_C = 0.8(0.05) = 0.04$$

For the functional failure mode, the north-south spectral ratio at the basemat at the front-to-back direction is 0.77. Therefore, the median factor of safety is

$$\hat{F}_{GMI} = \frac{1}{0.77} = 1.30$$

From the methodology discussed in Reference 1, the composite variability and the constituent randomness and uncertainty β values are evaluated as

$$\beta_{GMI_C} = \left[0.05^2 + \left(\frac{1}{2.33}\ln 1.30\right)^2\right]^{1/2} = 0.12$$

$$\beta_{GMI_R} = 0.6(0.12) = 0.07$$

$$\beta_{GMI_U} = 0.8(0.12) = 0.10$$

Overall Structural Response Factor

Combining the contributions of the Structural Spectral Shape and Ground Motion Incoherency, the overall Structural Response factor and its variabilities are

Structural $\hat{F}_{SR} = 1.00$

$$\beta_{SR_R} = (0.29^2 + 0.03^2)^{1/2} = 0.29$$

$$\beta_{SR_U} = (0^2 + 0.04^2)^{1/2} = 0.04$$

Functional $\quad \hat{F}_{SR} = 1.30$

$$\beta_{SR_R} = (0.24^2 + 0.07^2)^{1/2} = 0.25$$

$$\beta_{SR_U} = (0^2 + 0.10^2)^{1/2} = 0.10$$

Ground Spectral Acceleration Capacity

The median ground spectral acceleration capacities and their associated variabilities for the structural and functional failure modes of the Diesel Generator Control Panel are evaluated as

Structural

$$\bar{S}_a = (2.02)(1.00)(1.00)(2.00g)(1.125) = 4.55g$$

$$\beta_R = (0.05^2 + 0.06^2 + 0.29^2)^{1/2} = 0.30$$

$$\beta_U = (0.11^2 + 0.06^2 + 0.04^2)^{1/2} = 0.13$$

Functional

$$\bar{S}_a = (2.99)(1.00)(1.30)(2.00g)(1.125) = 8.74$$

$$\beta_R = (0.0^2 + 0.06^2 + 0.25^2)^{1/2} = 0.25$$

$$\beta_U = (0.08^2 + 0.05^2 + 0.10^2)^{1/2} = 0.14$$

## REFERENCES


1. Kipp, T.K., Wesley, D.A., Nakaki, D.K., and Kennedy, R.P., **Seismic Fragilities of Civil Structures and Equipment Components at the Diablo Canyon Power Plant,** NTS Engineering Report No. 1643.02, Revision 0, January, 1989.

2. **An Evaluation of the Yield, Tensile, Creep, and Rupture Strengths of Wrought 304, 316, 321, and 347 Stainless Steels at Elevated Temperatures,** ASTM DS 552, American Society of Testing Materials.

3. Kennedy, R.P., et. al., **Engineering Characterization of Ground Motion, Effects of Characteristics of Free-Field Motion on Structural Response,** NUREG/CR-3805, May, 1984.

4. Riddell, R. and Newmark, N.M., **Statistical Analysis of the Response of Nonlinear Systems Subjected to Earthquakes,** Department of Civil Engineering, Report UILU 79-2016, Urbana, Illinois, August, 1979.

5. Kennedy, R.P., et. al., **Subsystem Response Review, Seismic Safety Margins Research Program,** NUREG/CR-1706, July, 1981.

6. Kennedy, R.P., et. al., **Subsystem Fragility, Seismic Safety Margins Research Program (Phase I),** NUREG/CR-2405, February, 1982.

7. Kennedy, R.P., et. al., **Engineering Characterization of Ground Motion, Task II,** NUREG/CR-3805, Vol. 2, March, 1985.

8. **Shake Table Relay Ruggedness Tests, Test Series No. 1,** ANCO Engineers, Inc., Prepared for Electric Power Research Institute, April, 1988.

ENCLOSURE 2

REPORT NO. 11-0170-0031, "ADDITIONAL NONLINEAR TIME-HISTORY ANALYSES FOR DIABLO CANYON TURBINE BUILDING," IMPELL CORPORATION, MAY 1989

11-0170-0031

# ADDITIONAL NONLINEAR TIME-HISTORY ANALYSES FOR DIABLO CANYON TURBINE BUILDING

Prepared for

PACIFIC GAS & ELECTRIC COMPANY
77 Beale Street
San Francisco, California 94106

by

R. P. Kennedy
M. W. Salmon
D. K. Nakaki

May 1989

IMPELL CORPORATION

IMPELL CORPORATION

# REPORT APPROVAL COVER SHEET

CLIENT: PACIFIC GAS & ELECTRIC COMPANY

PROJECT: DIABLO CANYON LONG-TERM SEISMIC PROGRAM SUPPORT

JOB NUMBER(S): 0170-129-1831

REPORT TITLE: ADDITIONAL NONLINEAR TIME-HISTORY ANALYSES FOR DIABLO CANYON TURBINE BUILDING

REPORT NUMBER: 11-0170-0031

## REVISION RECORD

| REV. | PREPARED | REVIEWED | APPROVED | DATE |
|---|---|---|---|---|
| 0 | Robert P. Kennedy<br>Robert P. Kennedy | Thomas L. Kipp | Thomas L. Kipp | 5/23/89 |

Effective 06/88

# TABLE OF CONTENTS

# LIST OF TABLES

## Introduction

Reference 1 describes a series of nonlinear time-history analyses conducted on an analytical model used to define the lateral drift of the major east-west load-carrying shear walls (Walls 19 and 31) of the Diablo Canyon Turbine Building. To account for the variability of ground motion characteristics, a total of 25 different earthquake ground motion time-histories were used (listed in Table 3.1 of Ref. 1). Each time-history was scaled to have the same average 5% damped spectral acceleration ($\overline{S}_a$) over the 3.0 to 8.5 Hz frequency range. Twenty-five nonlinear time-history analyses were performed at both $\overline{S}_a = 3.0g$ and $\overline{S}_a = 6.0g$ using median structure properties. The results of these analyses were used to develop a median (randomness only) fragility estimate defining the median (randomness only) probability of severe shear wall distress as a function of $\overline{S}_a$. In addition, observations were made on various aspects of the nonlinear response of the Turbine Building and on the influence of ground motion characteristics on shear wall drift. Next, 50 sets of randomly selected structure damping, stiffness, and strength properties were developed (Table 2-7 of Ref. 1) to study the influence of uncertainty of structure properties on shear wall distress. Fifty nonlinear analyses (using each of the 25 input time-histories twice) were performed at $\overline{S}_a = 3.0g$, 4.0g, and 6.0g each. These analyses were used to develop fragility estimates which incorporated both uncertainty in structure properties and randomness of input motion (Equation 6.1 of Ref. 1). In addition, ground motion 5% damped response spectral acceleration limits were established (Equation 7.1 of Ref. 1) below which there is High-Confidence-of-Low-Probability-of-Failure (HCLPF) of the Turbine Building.

A possible issue concerning these studies described in Reference 1 is that these studies were conducted at very high ground motion levels ($\overline{S}_a$ = 3.0 to 6.0g), whereas a significant portion of the reported seismic risk of severe Turbine Building distress comes from ground motion centered on about $\overline{S}_a = 2.25g$ (Ref. 2). To address this issue, an additional series of nonlinear analyses have been performed at $\overline{S}_a = 2.25g$, following the methodology of Reference 1. The results of these analyses are summarized in this brief report. Based on these additional analyses, the observations, fragility estimates (Equation 6.1), and HCLPF Spectral Limits (Equation 7.1) of Reference 1 were found to be equally appropriate for $\overline{S}_a$ = 2.25g.

**Median (Input Randomness Only) Nonlinear Analyses at $\overline{S}_a$ = 2.25g**

Table 5-1 of Reference 1 shows that for a median structural model, only 3 trials (Trials 15, 18, and 20) at $\overline{S}_a$ = 3.0g produced maximum story drifts in excess of 0.5% (i.e., are capable of producing severe shear wall distress considering input randomness only). The total drift at the top of the shear walls (operating floor level) and the maximum story drift for those 3 trials were substantially greater than for any of the other 22 trials. Furthermore, both the operating floor and turbine pedestal drifts were substantially greater for Trial 15 than for any of the other 24 trials at $\overline{S}_a$ = 3.0g. Therefore, it is reasonable to assume that, at $\overline{S}_a$ = 2.25g, one of those 3 trials will produce the largest shear wall top drift and maximum story drift, and the largest operating floor and turbine pedestal drifts. For this reason, Trials 15, 18, and 20 with median structural properties were rerun at $\overline{S}_a$ = 2.25g, and the results are summarized in Table 1. With median structural properties, the probability of severe wall distress was negligible (computed to be zero) at $\overline{S}_a$ = 3.0g for each of the other 22 trials, so that no useful purpose would be served by rerunning these other trials at $\overline{S}_a$= 2.25g. The following points should be noted:

1. The largest total drift at the top of the shear walls was only 0.84 inches, or 0.13% of the wall height of 55 feet. The maximum story drift was only 0.26% of the story height. These drifts are substantially too low to conceivably produce severe shear wall distress with median structural properties. Thus, at $\overline{S}_a$ = 2.25g, the median (randomness only) probability of severe shear wall distress is zero.

2. None of these trials produced pedestal impact. Therefore, at $\overline{S}_a$ = 2.25g with median structural properties, it is very unlikely for the operating floor to impact the turbine pedestal. In Trial 15, the operating floor drift was about 1.15 times the available gap size (3.375 inches), and the square-root-sum-of-squares (SRSS) combination of operating floor and turbine pedestal drifts was 1.48 times the gap size. In Trial 20, the SRSS combined drift was 1.08 times the gap size. Yet, no impacts occurred. The observations made in Section 7.3 and Equation 5.2 of Reference 1 concerning pedestal impact are supported by these $\overline{S}_a$ = 2.25g analyses.

**Nonlinear Analyses with Uncertain Structure Properties at $\overline{S}_a$ = 2.25g**

In Reference 1, it was observed that even with varying structural properties, nonlinear trials for which the input ground motion spectral accelerations exceeded the limits of Equation 7.1 were the only ones capable of producing shear wall maximum story drifts in excess of 0.4% of the story height. When scaled to $\overline{S}_a$ = 2.25g, only Records 2, 5, 6, 9, 15, 16, 17, 18, 20, 23, and 24 exceed the limits of Equation 7.1 of Reference 1. Therefore, at $\overline{S}_a$ = 2.25g, only those trials which use these records are likely to produce the larger maximum story drifts. However, not all 22 trials which use these 11 records will produce the larger maximum story drifts. As noted in Section 6.5 of Reference 1, it is necessary to couple a record which exceeds the limits of Equation 7.1 with a structural model which has relatively lower shear wall stiffness and strength estimates as defined in Table 2.7 of Reference 1. To incorporate this shear wall stiffness and strength influence, only trials which produced greater than 0.4% maximum story drifts at $\overline{S}_a$ = 3.0g were rerun. Trials which use the above listed 11 records and also produced maximum story drifts greater than 0.40% when scaled to $\overline{S}_a$ = 3.0g, as shown in Table 6.1 of Reference 1, were Trials 2, 15, 16, 17, 18, 20, 31, 40, 41, 42, and 43. These 11 trials out of the total of 50 trials are most likely to produce the largest shear wall drifts when scaled to $\overline{S}_a$ = 2.25g. All of these 11 trials were rerun at $\overline{S}_a$ = 2.25g. These are the only 11 trials which might be expected to produce a maximum story drift in excess of 0.25% at $\overline{S}_a$ = 2.25g, and thus, exhibit greater than essentially zero probability of severe shear wall distress based upon the drift criteria defined by Equation 2.5 of Reference 1. Therefore, it was judged that these 11 trials were the only trials which needed to be rerun at $\overline{S}_a$ = 2.25g, and that rerun of the other trials was unnecessary. However, 4 other trials (Trials 13, 22, 25, and 26) produced maximum story drifts greater than 0.40% when scaled to $\overline{S}_a$ = 3.0g. To check the premise that the largest shear wall drifts will be produced by some of the previous 11 trials, Trials 13 and 26 from this later group were also run at $\overline{S}_a$ = 2.25g. It will be shown that these later two trials produce maximum story drifts less than 0.25%, whereas 5 of the previous 11 trials produce maximum story drifts well in excess of 0.25% when scaled to $\overline{S}_a$ = 2.25g, thus confirming the previous premise. It is virtually certain that these 5 trials are the only trials out of the total of 50 trials which produce maximum story drifts in excess of 0.25% when scaled to $\overline{S}_a$ = 2.25g.

At $\overline{S}_a$ = 3.0g, pedestal impact occurred (Table 6.1 of Ref. 1) for 18 of the 50 trials (36%). The 13 trials described above include 9 of those 18 pedestal impact cases. Based upon a previous extrapolation of the $\overline{S}_a$ = 3.0g results down to $\overline{S}_a$ = 2.25g, it was estimated that pedestal impact would be likely for 4 trials (Trials 31, 40, 42, and 43) and possible for two other trials (Trials 22 and 25) at $\overline{S}_a$ = 2.25g. All 4 of the likely cases were included in the 13 trials run at $\overline{S}_a$ = 2.25g.

The results for the 13 trials analyzed at $\overline{S}_a$ = 2.25g are summarized in Table 2. Only 4 trials out of the original 50 trials (8%) produced maximum story drifts in excess of 0.4% of the story height, or total drifts at the top of the shear walls in excess of 1.3 inches (0.2% of the wall height). These 4 trials were both of the trials which used input Records 15 and 17. These 4 trials were also the trials which produced the largest drifts at $\overline{S}_a$ = 3.0g. The observations made in Sections 3 and 7.2 of Reference 1 concerning the possible conservatism introduced by including input Records 15 and 17 also apply to an even greater extent at $\overline{S}_a$ = 2.25g. As noted in Table 3.1 and discussed in Sections 3 and 7.2, of Reference 1, Records 15 and 17 were frequency-dependent scaled to make them more applicable to the Diablo Canyon site. This frequency-dependent scaling both increased their overall amplitudes, and also enriched their lower frequency content (below 3 Hz). It is believed that this lower frequency enrichment greatly contributed to the large drifts computed from these two records. None of the records which did not undergo frequency-dependent scaling produced maximum story drifts in excess of 0.16% when scaled to $\overline{S}_a$ = 2.25g. The composite (randomness plus uncertainty) probability of severe shear wall distress of 2.9% at $\overline{S}_a$ = 2.25g computed in Table 2 would be reduced to essentially zero percent if the 4 trials that used Records 15 and 17 were removed. At $\overline{S}_a$ = 2.25g, essentially all of the risk of severe shear wall distress comes from Records 15 and 17. None of the other records are capable of severely distressing the Turbine Building shear walls at this ground motion level.

In 6 trials, either the operating floor or turbine pedestal drift exceeds the gap size (3.375 inches). Impact occurs in only 4 of these cases. Impact does not occur in any case where neither the turbine pedestal nor operating floor drift exceeds the gap size. For the 37 trials not rerun at $\overline{S}_a$ = 2.25g, impact appears to be possible in only 2 additional trials (Trials 22 and 25) at $\overline{S}_a$ = 2.25g. Thus, the likelihood of impact at $\overline{S}_a$ = 2.25g is about 8% to 12% of the 50 trials. These findings are consistent with the observations reported in Section 7.3 of Reference 1. As noted in Sections 5.1 and 7.3 of Reference 1, impact between the operating

floor and the turbine pedestal is primarily due to the operating floor drifting into contact with the turbine pedestal. Thus, the turbine pedestal tends to stabilize the operating floor and prevent it from drifting further. Impact has no negative influence and possibly some beneficial influence on shear wall distress.

## Comparison of Results with Fragility Estimate at $\overline{S}_a = 2.25g$

Equation 6-1 of Reference 1 provides a lognormally distributed fragility estimate which was fit to the 200 nonlinear time-history analyses conducted in the $\overline{S}_a = 3.0g$ to 6.0g range. Table 3 presents the predicted probability of severe shear wall distress at $\overline{S}_a = 2.25g$ obtained from Equation 6.1 for both the Randomness-Only and Composite (Randomness plus Uncertainty) cases. Also shown in Table 3 are the probabilities obtained from the nonlinear analyses conducted at $\overline{S}_a = 2.25g$. Note the excellent agreement.

## Conclusions

Extrapolation of the Turbine Building fragility estimate, the HCLPF Spectral Limits, and all observations contained in Reference 1 down to $\overline{S}_a = 2.25g$ are fully supported by the nonlinear analyses conducted at $\overline{S}_a = 2.25g$ which are summarized in this brief report.

## References

1. Kennedy, R. P., D. A. Wesley, and W. H. Tong, **Probabilistic Evaluation of the Diablo Canyon Turbine Building Seismic Capacity Using Nonlinear Time-History Analyses**, Report Number 1643.-01, NTS Engineering, December 1988.

2. **Final Report of the Diablo Canyon Long-Term Seismic Program**, Pacific Gas and Electric Company, July 1988.

TABLE 1

NONLINEAR RESULTS FOR MEDIAN STRUCTURAL MODEL AT $\overline{S}_a = 2.25g$

| Trial No. | Wall 19 | | Wall 31 | | Operating Floor Drift (inches) | Turbine Pedestal Drift (inches) | Pedestal Impact |
|---|---|---|---|---|---|---|---|
| | Top Drift (inches) | Maximum Story Drift (%) | Top Drift (inches) | Maximum Story Drift (%) | | | |
| 15 | 0.74 | 0.24 | 0.84 | 0.26 | 3.88 | 3.16 | No |
| 18 | 0.48 | 0.15 | 0.53 | 0.15 | 2.75 | 1.86 | No |
| 20 | 0.61 | 0.19 | 0.76 | 0.24 | 2.75 | 2.38 | No |

## TABLE 2

## NONLINEAR RESULTS FOR UNCERTAIN STRUCTURAL PROPERTIES AT $\overline{S}_a$ = 2.25g

| Trial No. | Wall 19 | | Wall 31 | | Prob. Severe Distress (%) | Operating Floor Drift (inches) | Turbine Pedestal Drift (inches) | Pedestal Impact |
|---|---|---|---|---|---|---|---|---|
| | Top Drift (inches) | Maximum Story Drift (%) | Top Drift (inches) | Maximum Story Drift (%) | | | | |
| 2 | 0.36 | 0.08 | 0.49 | 0.15 | 0 | 1.98 | 3.11 | - |
| 13 | 0.65 | 0.19 | 0.73 | 0.22 | 0 | 2.92 | 2.05 | - |
| 15 | 1.13 | 0.32 | 1.37 | 0.41 | 5.5 | 5.05 | 5.15 | - |
| 16 | 0.92 | 0.27 | 1.00 | 0.33 | 1.3 | 1.82 | 1.45 | - |
| 17 | 2.02 | 0.39 | 2.14 | 0.56 | 25.1 | 2.46 | 0.83 | - |
| 18 | 0.12 | 0.02 | 0.14 | 0.03 | 0 | 2.42 | 3.65 | - |
| 20 | 0.47 | 0.16 | 0.50 | 0.16 | 0 | 2.30 | 0.68 | - |
| 26 | 0.43 | 0.06 | 0.58 | 0.14 | 0 | 2.36 | 2.51 | - |
| 31 | 0.56 | 0.06 | 0.77 | 0.16 | 0 | 3.97 | 1.06 | Yes |
| 40 | 1.80 | 0.47 | 1.97 | 0.61 | 34.1 | 4.33 | 2.96 | Yes |
| 41 | 0.37 | 0.11 | 0.38 | 0.11 | 0 | 2.93 | 2.41 | - |
| 42 | 2.83 | 0.63 | 3.42 | 0.94 | 81.1 | 5.17 | 2.77 | Yes |
| 43 | 0.40 | 0.11 | 0.58 | 0.22 | 0 | 2.40 | 5.77 | Yes |
| | | | | | $\Sigma$ = 147.1 | | | |

$$P_F = \frac{147.1}{50} = 2.9\%$$

## TABLE 3

## COMPARISON OF PREDICTED AND COMPUTED PROBABILITY OF SEVERE WALL DISTRESS ESTIMATES AT $\overline{S}_a = 2.25g$

| | Predicted Eqn. 6-1, Ref. 1 $P_F$ (%) | Computed from Nonlinear Analyses $P_F$ (%) |
|---|---|---|
| Randomness Only | 0.1 | 0. |
| Composite (Randomness + Uncertainty) | 2.7 | 2.9 |